THE ASTROPHYSICAL JOURNAL, 507:919–937, 1998 November 10

MEASUREMENTS OF STARSPOT PARAMETERS ON ACTIVE STARS USING MOLECULAR BANDS IN ECHELLE SPECTRA

DOUGLAS O'NEAL[1,2]
Department of Astronomy and Astrophysics, The Pennsylvania State University, 525 Davey Laboratory, University Park, PA 16802; doneal@casa.colorado.edu

JAMES E. NEFF
Department of Physics and Astronomy, College of Charleston, Charleston, SC 29424; neffj@cofc.edu

STEVEN H. SAAR
Harvard/Smithsonian Center for Astrophysics, 60 Garden Street, Cambridge, MA 02138; saar@cfa.harvard.edu
Received 1997 September 11; accepted 1998 June 17

ABSTRACT

We present results from a study of starspot areas (f_S) and temperatures (T_S), primarily on active, single-lined spectroscopic binaries, determined using molecular absorption bands. Expanding upon our previous studies, we have analyzed multiorder echelle spectra of eight systems to simultaneously measure several different molecular bands and chromospheric emission lines. We determined starspot parameters by fitting the molecular bands of interest, using spectra of inactive G and K stars as proxies for the nonspotted photosphere of the active stars, and using spectra of M stars as proxies for the spots. At least two bands with different $T_{\rm eff}$ sensitivities are required. We found that fitting bands other than the TiO 7055 and 8860 Å features does not greatly extend the temperature range or sensitivity of our technique. The 8860 Å band is particularly important because of its sharply different temperature sensitivity. We did not find any substantial departures from f_S or T_S that we have measured previously based on single-order spectra. We refined our derived spot parameters using contemporaneous photometry where available. We found that using M giants as spot proxies for subgiant active stars often underestimates f_S needed to fit the photometry; this is presumably due to the increase in strength of the TiO bands with decreasing gravity. We also investigated correlations between f_S and chromospheric emission, and we developed a simple method to measure nonspot temperature (T_Q) solely from our echelle spectra.

Subject headings: binaries: spectroscopic — stars: activity — stars: fundamental parameters — stars: late-type — stars: spots

1. INTRODUCTION

In previous papers in this series (Neff, O'Neal, & Saar 1995, hereafter Paper I; O'Neal, Saar, & Neff 1996, hereafter Paper II), we describe a technique using the absorption bands of the titanium oxide molecule near 7055 Å [the 7055, 7088, and 7126 Å bands of the $\gamma(0, 0)$ system] and the band at 8860 Å [the strongest of the $\delta(0, 0)$ system] to measure the temperature and area of dark, cool starspots in the photospheres of magnetically active stars. We use spectra of inactive M stars to model the spotted regions of active star photospheres and spectra of inactive G and K stars to model the unspotted regions. These proxy spectra are weighted by their relative continuum fluxes and by a surface-area–filling factor to reproduce spectra of the active star. In Papers I and II we measure the depths of the 7055 and 8860 Å TiO absorption bands in five active stars; using empirical depth versus $T_{\rm eff}$ relations from inactive stars, we computed the spot area and temperature (T_S) needed to reproduce the measured band depths in the active star spectra. Using that technique, the ratio of the depths of these bands in an active star spectrum is a function of T_S, while the absolute depth of each band is a function of the total projected area of starspots on the visible hemisphere, f_S.

Traditionally, photometric light-curve modeling has been used to measure properties of starspots (e.g., Strassmeier, Hall, & Henry 1994). That technique can only measure an asymmetric spot distribution or differences from a presumed "immaculate" (unspotted) light level. A symmetric distribution, either a monolithic polar spot or smaller spots spread evenly in longitude, will produce no variation of the star's brightness. More spatial detail can be derived using Doppler imaging, in which asymmetries in a line profile from a rapidly rotating star are used to model the asymmetries on the stellar surface (e.g., Piskunov, Tuominen, & Vilhu 1990; Strassmeier et al. 1991; Hatzes & Vogt 1992). In contrast, our spectroscopic technique can detect starspots even on a slowly rotating star, without regard to their spatial distribution.

In this paper, we further develop our technique in two significant ways. First, we have obtained multiorder echelle spectra of our active targets and comparison stars. These spectra show many molecular bands, including the 4760, 4950, 5168, 6158, and 6650 Å bands of TiO; the 5500 Å band of CaOH; and the 4845 Å band of MgH, in addition to the 7055 and 8860 Å TiO bands. Second, instead of simply measuring the depths of the bands as before, we have used our grids of inactive star spectra to fit entire echelle orders containing bands in active star spectra. We had several goals. By observing many molecular bands of different and wider $T_{\rm eff}$ sensitivities, we hoped to extend the T_S range over which our technique is applicable (the two TiO bands used in Papers I and II are too weak for $T_S > 4000$ K). We also hoped that fitting the multiple bands would

[1] Current address: JILA, University of Colorado, Campus Box 440, Boulder, CO 80309-0440.

[2] Visiting Astronomer, Kitt Peak National Observatory, National Optical Astronomy Observatories, operated by AURA, Inc., under cooperative agreement with the National Science Foundation.

better determine T_S and permit a search for multiple starspot temperatures. By comparing spectra of active and inactive stars in orders relatively unaffected by molecular bands, we planned to constrain the unspotted photospheric temperature, T_Q, spectroscopically (unlike Papers I and II, where photometry was needed). Finally, echelle spectroscopy allows simultaneous monitoring of chromospheric activity indicators, such as Hα, Ca II H and K, and the Ca II infrared triplet, enabling us to test whether the strength of chromospheric emission is correlated with f_S.

2. OBSERVATIONS AND ANALYSIS

2.1. *The Data*

The data were obtained during two observing runs at the Coudé Feed Telescope at Kitt Peak National Observatory using the Penn State Fiber Optic Echelle Spectrograph (FOE), during one run at the 2.1 m Otto Struve Telescope at McDonald Observatory using the Sandiford Cassegrain Echelle Spectrograph, and during 2 yr at the 1.6 m telescope at Penn State's Black Moshannon Observatory (BMO) using the QDSS Echelle Spectrograph.

The FOE (Ramsey & Huenemoerder 1986) in Quasi-Littrow mode, prism cross-dispersed, yields a resolution $R = \lambda/\Delta\lambda \approx 14{,}000$. We used a 1024×1024 Tektronix CCD with 24 μm pixels for the 1992 March observing run. In 1995 January we used a 3 K × 1 K Loral CCD with 15 μm pixels. In both cases, the spectra cover from 3800 to 9000 Å, with gaps of up to 60 Å for $\lambda \geq 7500$ Å. We also reanalyze FOE data of II Peg from 1991 October (Byrne et al. 1995). The FOE spectra typically had a signal-to-noise ratio (S/N) ~ 60–80 at the longest wavelengths, improving toward shorter λ to S/N ≳ 120 at Hα and the 7055 Å TiO bands.

The Sandiford Cassegrain Echelle Spectrograph (McCarthy et al. 1993) at the McDonald Observatory 2.1 m telescope offers higher resolution ($R \approx 60{,}000$) than the FOE but more limited wavelength coverage. In 1995 December we used this instrument with a Reticon 1200×400 CCD with 27 μm pixels. The spectrograph operates close to true Littrow and uses prism cross-dispersion. The spectra we obtained cover from Hα to past the 8860 Å TiO band, with no wavelength gaps shortward of 8500 Å. As for the FOE spectra, the McDonald observations had S/N ≳ 100 in the orders containing Hα and the 7055 Å TiO bands, and S/N ~ 50–80 in the orders containing the Ca II IRT and the 8860 Å TiO band.

At BMO, between 1992 August and 1994 October we obtained 22 spectra of II Peg, along with spectra of other active stars and our comparison star grids. The QDSS is grating cross-dispersed and gives $R \approx 6000$. Until 1994 February the QDSS used a 320×512 RCA CCD, which was then replaced by an 800×800 TI CCD. In the original configuration, the 8860 Å TiO band head fell too close to the edge of the CCD for useful observations. The spectral coverage was from ≈4900 to 9000 Å, 80 ≲ S/N ≲ 150. In all three systems, we used Th-Ar lamps for wavelength calibration and various quartz lamps for flat-fielding.

The active stars observed in this program are listed in Table 1, along with an ephemeris and reference for each. We also list our derived T_Q and T_S values for each active star. Our observations of the active stars are listed in Table 2, along with the f_S computed for each spectrum. Table 3 lists the properties of the comparison stars observed for this program. When selecting comparison stars, we searched for bright, minimally variable stars with low activity, and we avoided stars that appear to be very metal-poor or metal-rich. Photometry for the stars comes from Stauffer & Hartmann (1986) and the Bright Star Catalog (Hoffleit & Jaschek 1982). Values of $T_{\rm eff}$ for the M giants and cooler K giants ($T_{\rm eff} \leq 4400$ K) were computed from the $T_{\rm eff}$ versus $(V-K)$ calibration by Ridgway et al. (1980); for the warmer giants, we used the $T_{\rm eff}$ versus $(B-V)$ calibration by Böhm-Vitense (1980). We used the $T_{\rm eff}$ versus $(R-I)_{\rm KC}$ relation by Bessell (1991) for the M dwarfs, and an average of a $T_{\rm eff}$ versus $(B-V)$ relation (Gray 1988) and a $T_{\rm eff}$ versus $(R-I)_J$ color relation (Johnson 1966) for the G and K dwarfs. The computed $T_{\rm eff}$ values were rounded to the nearest interval of 25 K. In Table 3, check marks indicate with which instruments we observed each star.

We used the REDUCE echelle package (Hall et al. 1994) for data reduction. Bias removal, creation of order maps, flat-field division, scattered-light removal, and extraction of the spectra were performed as described by Hall et al. (1994). Wavelength calibration was accomplished by marking positions of Th-Ar lines in each echelle order, then doing a two-dimensional, second-order calibration of the entire frame. The last step using REDUCE was the crude normalization of all spectral orders, done by fitting a cubic spline to a relatively featureless spectrum (e.g., of a hot star) and dividing each object spectrum by that fit order-by-order. For orders containing spectral features of interest, more careful normalization was done by fitting a spline to the stellar continuum. Telluric lines were removed by the

TABLE 1

PARAMETERS AND EPHEMERIDES FOR ACTIVE STARS

Star	HD	Spectral Type	$P_{\rm rot}$ (days)	Date[a] (for $\phi = 0$[c])	T_Q[b] (K)	T_S (K)
II Peg	224085	K2–3 IV–V	6.72422	3033.47	4750	3530 ± 100
EI Eri	26337	G5 IV	1.945	4635.65	5600	3700 ± 150
V1762 Cyg.....	179094	K2 III–IV	28.5895	2479.214	4600 ± 150	3500 ± 150
V1794 Cyg.....	199178	G5 III–IV	3.337484	4395.780	5350	3800 ± 200
σ Gem	62044	K1 III	19.60447	7227.08	4600 ± 200	3850 ± 100
DM UMa	...	K0–1 III–IV	7.4949	7623.383	4600 ± 150	3570 ± 100
HU Vir	106225	K0 IV	10.38758	8375.25	5000 ± 150	3440 ± 100
λ And	222107	G8 III–IV	53.95	3829.20	4750	3650 ± 150

[a] HJD: 2,440,000.

[b] T_Q values without uncertainties are assumed from previous work.

[c] References for ephemerides: II Peg, Vogt (1981); EI Eri, Strassmeier (1990); V1762 Cyg, Strassmeier et al. (1994); V1794 Cyg, Jetsu et al. (1990); σ Gem, Bopp & Dempsey (1989); DM UMa, Strassmeier et al. (1993); HU Vir, Fekel et al. (1986); λ And, Boyd et al. (1983).

"drying" procedure described in Paper I. All data from spectral orders containing features of interest were interpolated onto common wavelength scales.

2.2. *Characteristics of Molecular Bands*

In Figure 1 we illustrate the variations of the strengths of various bands with $T_{\rm eff}$. These measurements were made by fitting lines to the pseudocontinua blueward of the band heads and to the residual intensity values inside the bands. We then measured the band depth relative to the normalized continuum intensity at the band head wavelength. We also measured the bands in spectra of M dwarf comparison stars; as found in Papers I and II for the 7055 and 8860 Å TiO bands, the molecular bands are weaker at a given $T_{\rm eff}$ in spectra of M dwarfs than in M giants. The differing resolution of the three spectrographs used does not appreciably change the measured band depths except in a few of the shorter wavelength bands where low S/N made measurements uncertain for the BMO/QDSS spectra. Table 4 lists all the bands we measured in our echelle spectra of M giant comparison stars, along with the depth of each in BY Boo ($T_{\rm eff} = 3550$ K).

We next searched for other molecular absorption features that might remain strong above $T_{\rm eff} = 4000$ K (the upper limit for the bands used in Papers I and II; see Fig. 2 of Paper II). The TiO band at 5166 Å [the strongest of the $\alpha(0, 0)$ system] exhibits a depth of $\approx 40\%$ in our warmest M giant comparison stars ($T_{\rm eff} = 3950$ K), while several bands, including the TiO band at 6158 Å, are still 20% deep. Unfortunately, a closer examination of the regions of these two band heads in our late-K giant comparison stars shows that neither the 5166 Å band nor the 6158 Å band remains strong in stars as warm as ν UMa ($T_{\rm eff} = 4200$ K). The same is true of the other bands we measured; the 4000 K upper limit found for the 7055 Å TiO bands therefore also applies to other TiO features.

To be useful for measuring spot parameters, a molecular band must not only be intrinsically strong, but the ratio of the spot and photospheric continuum fluxes at that wavelength, R_λ, must be great enough to produce a measurable effect in the spectrum. To compute R_λ for a given star, we use models by Kurucz (1991), selecting the models whose $\log g$ values are closest to the star's estimated gravity. The relationship between $\log (T_{\rm eff})$ and $\log (\langle F_C \rangle)$,

TABLE 2

ECHELLE SPECTRAL OBSERVATIONS OF ACTIVE STARS

Star	Date	Instrument[a]	JD (mid)[b]	Phase (mid)	f_S
II Peg	1991 Oct 12	FOE/CF	8541.65	0.15	0.45 ± 0.04
	1991 Oct 13	FOE/CF	8542.82	0.33	0.49 ± 0.03
	1991 Oct 14	FOE/CF	8543.77	0.47	0.48 ± 0.04
	1991 Oct 15	FOE/CF	8544.76	0.62	0.47 ± 0.04
	1991 Oct 16	FOE/CF	8545.74	0.77	0.46 ± 0.04
	1992 Aug 2	BMO	8836.83	0.05	0.47 ± 0.06
	1992 Aug 3	BMO	8837.83	0.20	0.43 ± 0.04
	1992 Aug 6	BMO	8840.81	0.65	0.41 ± 0.07
	1992 Aug 7	BMO	8841.80	0.79	0.50 ± 0.05
	1992 Aug 12	BMO	8846.76	0.53	0.36 ± 0.06
	1992 Aug 19	BMO	8853.78	0.57	0.36 ± 0.06
	1992 Aug 20	BMO	8854.76	0.72	0.46 ± 0.04
	1992 Aug 22	BMO	8856.80	0.02	0.46 ± 0.05
	1992 Oct 14	BMO	8909.56	0.87	0.49 ± 0.03
	1992 Oct 27	BMO	8922.65	0.82	0.47 ± 0.04
	1992 Oct 28	BMO	8923.65	0.96	0.46 ± 0.05
	1993 Aug 22	BMO	9221.77	0.30	0.49 ± 0.03
	1993 Sep 12	BMO	9242.69	0.41	0.31 ± 0.06
	1993 Sep 14	BMO	9244.73	0.71	0.39 ± 0.05
	1993 Dec 17	BMO	9338.62	0.68	0.36 ± 0.05
	1995 Jan 19	FOE/CF	9736.60	0.86	0.35 ± 0.06
	1995 Jan 20	FOE/CF	9737.61	0.01	0.26 ± 0.08
	1995 Jan 21	FOE/CF	9738.65	0.17	0.30 ± 0.05
	1995 Jan 23	FOE/CF	9740.58	0.46	0.35 ± 0.05
	1995 Dec 21	McD/CEch	10,072.63	0.84	0.30 ± 0.10
	1995 Dec 26	McD/CEch	10,077.60	0.58	0.43 ± 0.10
EI Eri	1992 Mar 19	FOE/CF	8700.60	0.95	0.34 ± 0.05
	1992 Mar 20	FOE/CF	8701.64	0.48	0.34 ± 0.05
	1992 Mar 21	FOE/CF	8702.60	0.98	0.23 ± 0.08
	1992 Mar 23	FOE/CF	8704.60	0.01	0.32 ± 0.05
	1992 Mar 24	FOE/CF	8705.61	0.54	0.35 ± 0.06
	1992 Mar 25	FOE/CF	8706.60	0.04	0.36 ± 0.05
	1992 Mar 26	FOE/CF	8707.60	0.55	0.28 ± 0.04
	1995 Jan 18	FOE/CF	9735.70	0.13	≤ 0.12
	1995 Jan 19	FOE/CF	9736.66	0.63	0.18 ± 0.07
	1995 Jan 21	FOE/CF	9738.68	0.67	0.18 ± 0.07
	1995 Dec 21	McD/CEch	10,072.82	0.46	0.15 ± 0.06
	1995 Dec 25	McD/CEch	10,076.83	0.52	0.15 ± 0.06
V1762 Cyg.....	1993 Aug 19	BMO	9218.71	0.73	0.10 ± 0.05
	1993 Sep 14	BMO	9244.62	0.64	0.20 ± 0.05
	1994 Jun 11	BMO	9514.73	0.09	0.27 ± 0.06
	1994 Jul 2	BMO	9535.72	0.82	0.18 ± 0.07
	1994 Jul 17	BMO	9550.76	0.35	0.12 ± 0.04

TABLE 2—*Continued*

Star	Date	Instrument[a]	JD (mid)[b]	Phase (mid)	f_S
V1794 Cyg.....	1992 Mar 24	FOE/CF	8706.01	0.46	0.20 ± 0.06
	1992 Mar 25	FOE/CF	8707.01	0.76	0.22 ± 0.06
	1993 Sep 11	BMO	9241.65	0.95	0.29 ± 0.04
	1994 Jun 11	BMO	9514.76	0.78	0.28 ± 0.04
	1994 Jul 2	BMO	9535.78	0.08	≤ 0.10
σ Gem	1992 Mar 17	FOE/CF	8698.71	0.07	0.11 ± 0.03
	1992 Mar 19	FOE/CF	8700.70	0.17	0.10 ± 0.04
	1992 Mar 20	FOE/CF	8701.72	0.22	0.16 ± 0.03
	1992 Mar 21	FOE/CF	8702.70	0.27	0.10 ± 0.05
	1992 Mar 22	FOE/CF	8703.77	0.32	0.12 ± 0.04
	1992 Mar 23	FOE/CF	8704.71	0.37	0.15 ± 0.03
	1992 Mar 24	FOE/CF	8705.72	0.42	0.11 ± 0.03
	1992 Mar 25	FOE/CF	8706.69	0.47	0.16 ± 0.03
	1992 Mar 26	FOE/CF	8707.67	0.52	0.20 ± 0.03
	1995 Jan 18	FOE/CF	9735.77	0.97	0.04 ± 0.04
	1995 Jan 19	FOE/CF	9736.81	0.02	0.03 ± 0.04
	1995 Jan 21	FOE/CF	9738.77	0.12	0.05 ± 0.05
	1995 Jan 22	FOE/CF	9739.81	0.17	0.14 ± 0.03
	1995 Jan 23	FOE/CF	9740.79	0.22	0.14 ± 0.05
	1995 Dec 20	McD/CEch	10,071.91	0.11	0.15 ± 0.03
	1995 Dec 21	McD/CEch	10,072.88	0.16	0.18 ± 0.03
	1995 Dec 25	McD/CEch	10,076.88	0.36	0.30 ± 0.04
	1995 Dec 26	McD/CEch	10,077.82	0.41	0.27 ± 0.03
DM UMa	1995 Jan 19	FOE/CF	9736.86	0.99	0.30 ± 0.10
	1995 Jan 22	FOE/CF	9739.91	0.40	0.35 ± 0.08
	1995 Dec 25	McD/CEch	10076.96	0.37	0.25 ± 0.08
HU Vir	1995 Jan 23	FOE/CF	9740.93	0.70	0.44 ± 0.06
λ And	1993 Aug 22	BMO	9221.75	0.66	0.19 ± 0.08
	1993 Sep 14	BMO	9244.71	0.78	≤ 0.19
	1995 Jan 19	FOE/CF	9736.61	0.75	0.21 ± 0.06
	1995 Jan 20	FOE/CF	9737.62	0.80	0.23 ± 0.09
	1995 Jan 23	FOE/CF	9740.59	0.95	0.14 ± 0.07

[a] Instrument Key: FOE/CF = Fiber-Optic Echelle Spectrograph and 0.9 m Coudé Feed Telescope at Kitt Peak; BMO = QDSS Echelle Spectrograph and 1.6 m Black Moshannon Observatory Telescope; McD/CEch = Sandiford Cassegrain Echelle Spectrograph and 2.1 m Struve Telescope at McDonald Observatory.

[b] HJD: 2,440,000.

the average continuum flux in the given bandpass at the selected log g, is then approximated by a spline fit to the Kurucz values. To compute R_λ for 3500 K $> T_S \geq$ 3000 K, we extrapolate the cubic spline to lower $T_{\rm eff}$.

To test the utility of absorption bands other than those used in Papers I and II for measuring spot parameters, we chose the set of TiO bands near 6650 Å [the 6651, 6680, 6713, and 6746 Å bands of the γ(1,0) system], the TiO band at 6158 Å [the strongest of the γ'(0,0) system], and the 5166 Å feature. The strengths of the bands in the 6650 Å complex increase with decreasing temperature throughout the range of $T_{\rm eff}$ covered by our spot comparison stars. The 6158 Å band depth changes little for 3200 K $\leq T_S \leq$ 3500 K but becomes weaker for warmer $T_{\rm eff}$. The 5166 Å TiO band is blended with three strong Mg I absorption lines, which would introduce large uncertainties into any attempt to fit the molecular absorption. None of the bands of molecules other than TiO that we measured are both sufficiently strong in the spectra of mid-M giant stars and sufficiently far to the red to be useful (because R_λ is larger in the red) for measuring starspot parameters.

2.3. *Spectral Fitting Technique*

For fitting spectra of spotted stars in orders containing molecular bands of interest, we used the routine STARMOD, written (Barden 1985) and later modified by D. Huenemoerder, A. Welty, and one of us (D. O.) at Penn State. STARMOD fits an observed spectrum with a linear combination of up to three model spectra and has been used extensively (e.g., Welty & Wade 1995) to measure radial and rotational velocities, determine spectral types, and measure relative brightnesses of stars in systems of two or three components. We use this last function to find the relative weights of nonspot and spot components in spectra of active stars. STARMOD constructs a model by shifting a weighted standard star spectra in radial velocity and by applying a standard rotational broadening function (e.g., Gray 1988) with a limb-darkening coefficient $\epsilon = 0.6$. We shifted all spectra to a common wavelength scale and set the active star's $v \sin i$ to the best literature value prior to fitting. Thus, in our case, only the relative weights were iterated to achieve the best fit.

The best-fit relative weights of the two standard star spectra (the G/K "nonspot" comparison with $T_{\rm eff} = T_Q$ and the M "spot" comparison with $T_{\rm eff} = T_S$) computed by STARMOD are directly related to the starspot-filling factor on the active star. The normalized spectrum of the active star, $F_{\rm total}$, can be written as

$$F_{\rm total} = \frac{f_S R_\lambda F_S + (1 - f_S) F_Q}{f_S R_\lambda + (1 - f_S)}, \quad (1)$$

where f_S is the spot-filling factor, the total fractional projected area of spots on the observed hemisphere weighted by limb-darkening, and F_S and F_Q are the normalized comparison spectra for the spot and nonspot regions of the star, respectively. STARMOD calculates the best relative weights, W_S and W_Q, of the two comparison spectra, in such

a way that $F_{\rm total} = W_S F_S + W_Q F_Q$. Comparison with equation (1) implies that $W_Q = (1 - f_S)/[(f_S R_\lambda) + (1 - f_S)]$ and $W_S = (f_S R_\lambda)/[(f_S R_\lambda) + (1 - f_S)]$, and so we may write

$$f_S = \left(\frac{R_\lambda}{W_S} - R_\lambda + 1\right)^{-1}. \quad (2)$$

To test the ability of STARMOD to determine f_S and T_S on active stars, we first used a set of II Peg TiO band data that we had already analyzed by the band-depth technique (see Table 3 of Paper II). Using STARMOD, we fitted these II Peg spectra of the 7055 and 8860 Å TiO bands using McMath-Pierce comparison stars with $T_S = 3550$ K and $T_Q = 4825$ K. This produced results very similar to the band-depth method. Averaging the f_S values obtained by fitting the two bands (which differed from each other by 0.06 or less), the greatest difference between the STARMOD and band-depth measurements of f_S was 0.08 (on 1989 October 9). In only one other case was the difference greater than 0.05, and for the spectra of 1992 September the band depth and STARMOD measurements of f_S agreed to within 0.02 for all spectra. Given that the uncertainty (Paper II) for f_S measurements of II Peg was $\approx$0.05, we conclude that STARMOD provides at least as accurate a measurement of f_S for active stars as does the band-depth method.

To attempt to determine T_Q spectroscopically, we chose a spectral order relatively free of molecular bands (although no order, when observed in the coolest M giants, is completely band-free) and fitted spectra of each active star in that order using all the nonspot G and K giant comparison star spectra. The fit is primarily determined by the nonspot comparison spectrum. We chose the spectral order spanning from $\approx$6240 to 6410 Å, within which are found many temperature-sensitive lines of Fe I, as well as lines of Fe II, Si I, Si II, Cr I, Ti I, and V I. Results for these fits are presented in the subsections below for each active star. In addition to fitting the entire spectral order, we also attempted fits with the continuum masked out, i.e., using only pixels with values less than 95% (and in another trial, 90%) of the normalized continuum level. In general, these fits produced very similar results. Although not be able to fix T_Q as precisely as, e.g., careful analysis of high-resolution line profiles, this method can confirm and refine the proper T_Q range for our models.

In cases where we have previously computed T_S and T_Q for an active star, we chose comparison stars spanning

TABLE 3

PROPERTIES OF COMPARISON STARS

HD	HR	Name	Spectral Type	V	$(B-V)$	$(R-I)$	$T_{\rm eff}$	FOE	BMO	McD
Giant "Spot" Comparison Stars										
89758	4069	μ UMa	M0 III	3.1	1.59	0.96	3950	√		√
120477.....	5200	υ Boo	K5.5 III	4.1	1.52	0.87	3950	√		
60522	2905	υ Gem	M0 III	4.1	1.54	0.96	3925	√		√
80493	3705	α Lyn	K7 III	3.1	1.55	0.90	3925	√		√
189319.....	7635	γ Sge	M0 III	3.5	1.57	0.92	3925		√	
183439.....	7405	α Vul	M0 III	4.4	1.50	0.97	3825		√	
204724.....	8225	2 Peg	M1 III	4.6	1.62	1.09	3800		√	
183630.....	7414	36 Aql	M1 III	5.0	1.75	...	3800		√	
42995	2216	η Gem	M3 III	3.3	1.60	1.31	3650	√	√	
112300.....	4910	δ Vir	M3 III	3.4	1.58	1.33	3650	√		
217906.....	8775	β Peg	M2.5 II–III	2.4	1.67	1.32	3650		√	
29755	1496	54 Eri	M3.5 III	4.3	1.61	1.38	3625	√		√
44478	2286	μ Gem	M3 III	2.9	1.64	1.38	3625	√	√	
20720	1003	τ^4 Eri	M3.5 III	3.7	1.62	1.46	3600	√	√	√
2411	103	TV Psc	M3 III	5.1	1.65	1.54	3575	√	√	√
102620.....	4532	II Hya	M4 III	5.1	1.60	...	3550	√		
123657.....	5299	BY Boo	M4.5 III	5.3	1.59	1.66	3550	√	√	√
175588.....	7139	δ^2 Lyr	M4 II	4.3	1.68	1.63	3550	√	√	
113866.....	4949	FS Com	M5 III	5.6	1.59	1.81	3475	√	√	√
175865.....	7157	R Lyr	M5 III	4.0	1.59	1.91	3425	√	√	
172380.....	7009	XY Lyr	M5 II	6.0	1.65	1.96	3400	√	√	
94705	4267	VY Leo	M5.5 III	5.8	1.45	2.09	3325	√	√	√
18191	867	RZ Ari	M6 III	5.9	1.47	2.17	3200	√	√	√
41698	2156	S Lep	M6 III	7.0	1.63	2.37	3125	√		√
114961.....	...	SW Vir	M7 III	7.0	1.55	...	3100	√		
117287.....	5080	R Hya	M7 III	5.0	1.60	2.42	3050	√	√	√
Dwarf "Spot" Comparison Stars										
201092.....	8086	Gl 820B	K7 V	6.0	1.37	0.60	3850		√	
88230		Gl 380	K7 V	6.6	1.36	0.60	3825	√	√	
28343		Gl 169	K7 V	8.3	1.35	0.62	3750	√	√	
		Gl 186	K5 V	9.3	1.28	0.64	3725	√		
i11631		Gl 488	M0.5 Ve	8.5	1.40	0.66	3700	√	√	
79210		Gl 338A	M0 V	7.6	1.39	0.68	3675	√	√	
79211		Gl 338B	M0 V	7.7	1.42	0.69	3650	√	√	
32450		Gl 185A	M0 V	8.5	1.41	0.72	3625	√		
		Gl 400A	M2 V	9.3	1.41	0.74	3600	√	√	
		Gl 96	M1.5 Ve	9.4	1.49	0.78	3525		√	

TABLE 3—*Continued*

HD	HR	Name	Spectral Type	V	$(B-V)$	$(R-I)$	$T_{\rm eff}$	FOE	BMO	McD
42581		Gl 229A	M1 Ve	8.1	1.50	0.82	3450	√		
36395		Gl 205	M1.5 V	8.0	1.47	0.85	3400	√		
1326		Gl 15A	M2 V	8.1	1.56	0.88	3375	√	√	
95735		Gl 411	M2 Ve	7.5	1.51	0.91	3350	√	√	√
		Gl 393	M2.5 V	9.6	1.52	0.95	3325	√		
265866.....		Gl 251	M4 V	10.0	1.57	1.09	3250	√		
		Gl 273	M4 V	9.9	1.56	1.21	3175	√		
Giant "Non-Spot" Comparison Stars										
111812.....	4883	31 Com	G0 III	4.9	0.67	0.35	5650			√
41116	2134	1 Gem	G5 III	4.2	0.82	0.45	5250	√		√
21120	1030	o Tau	G6 III	3.6	0.89	0.45	5075	√		√
82635	3800	10 LMi	G8.5 III	4.6	0.92	0.46	5000	√		√
62345	2985	κ Gem	G8 III	3.6	0.93	0.45	4975	√		√
135722.....	5681	δ Boo	G8 III	3.5	0.95	0.51	4900	√		
82734	3808	...	K0 IV	5.0	1.02	...	4750	√		√
74442	3461	δ Cnc	K0 III	3.9	1.08	0.54	4625	√		√
73471	3418	σ Hya	K1 III	4.4	1.21	0.56	4600	√		√
95345	4291	58 Leo	K1 III	4.8	1.16	0.56	4600	√		
66216	3149	χ Gem	K1.5 III	4.9	1.12	...	4525	√		√
81146	3731	κ Leo	K2 III	4.5	1.23	0.63	4350	√		√
127665.....	5429	ρ Boo	K3 III	3.6	1.30	0.65	4300	√		√
98262	4377	ν UMa	K3 III	3.5	1.40	0.70	4200	√		√
69267	3249	β Cnc	K4 III	3.5	1.48	0.78	4050	√		√
Dwarf "Nonspot" Comparison Stars										
20630	996	κ^1 Cet	G5 Ve	4.8	0.68	0.36	5600	√	√	√
101501.....	4496	61 UMa	G8 Ve	5.3	0.72	0.36	5550	√	√	√
149661.....	6171	12 Oph	K2 V	5.8	0.82	0.39	5300	√	√	
185144.....	7462	σ Dra	K0 V	4.7	0.79	0.41	5300	√	√	
26965	1325	o^2 Eri A	K1 Ve	4.4	0.82	0.45	5175	√	√	√
22049	1084	ϵ Eri	K2 V	3.7	0.88	0.47	5050	√	√	√
160346.....	...	Gl 688	K3 V	6.5	0.96	0.50	4850	√	√	
16160	753	Gl 105A	K3 V	5.8	0.98	0.53	4775	√	√	√
32147	1614	Gl 183	K3 V	6.2	1.06	0.49	4750	√	√	√
131977.....	5568	Gl 570A	K4 V	5.8	1.11	0.56	4575	√	√	
201091.....	8085	61 Cyg A	K5 V	5.2	1.18	0.65	4325		√	

ranges of $T_{\rm eff}$ within ≈ 200 K of those temperatures. For the three stars for which we did not have previous temperature measurements (HU Vir, λ And, and DM UMa), we chose arrays of nonspot comparison stars spanning ~ 500 K, centered upon the approximate T_Q of the active star based on its colors, and arrays of spot comparison stars spanning the entire range 3000 K $\leq T_S \leq$ 4000 K. We then computed the best-fit f_S for using each spot/nonspot comparison star pair. For all fits using a given T_Q, we plotted T_S versus f_S for each echelle order fitted. Values of T_S and f_S for a given active star spectrum are then determined from where these fits for different bands intersect. In the following section, we present results from the implementation of this procedure for spectra of our eight active target stars.

3. RESULTS

3.1. *II Pegasi = HD 224085*

II Peg is a single-lined spectroscopic binary with a spectral type K2–3 IV–V and $v \sin i = 23$ km s^{-1} (consistent with recent Doppler imaging analysis by Hatzes 1995b). It is extremely active, exhibiting V-band variations of up to 0.6 mag (e.g., Byrne et al. 1995) and strong radio (Drake, Simon, & Linsky 1989) and X-ray (Dempsey et al. 1993b) activity. We previously found f_S values as high as 56% (Paper II).

We obtained four spectra of II Peg with the FOE in 1995 January. In these, the 7055 Å TiO band head fell close to the end of an order, with the first usable data at $\approx$7035 Å. We fitted wavelengths $\approx$7035–7150 Å for this order, encompassing all three strong bands of this system. The spectral regions used for fitting the other molecular bands were 8780–8900 Å for the 8860 Å TiO band, 6630–6750 Å for the 6650 Å system of TiO bands (including the band heads at 6650, 6680, and 6710 Å), and 6100–6200 Å for the 6158 Å band.

In Paper II, we found $T_Q = 4800$ K and $T_S = 3500$ K for II Peg. For our comparison star arrays, we used G/K stars spanning 4525 K $\leq T_{\rm eff} \leq$ 5250 K and M stars spanning 3325 K $\leq T_{\rm eff} \leq$ 3650 K. In Figure 2 we illustrate the best fits obtained for the II Peg spectrum of 1995 January 19 ($\phi = 0.86$) in each of the four orders fitted, when comparison stars with $T_Q = 4750$ K and $T_S = 3550$ K are used. Residuals are plotted at the bottom of each panel, with 0.1 added for ease of illustration.

Sample results of the STARMOD determinations of f_S are shown in Figure 3. For the 7055 Å order over this T_S range, f_S needed to fit the II Peg spectrum decreases with increasing T_S. This counterintuitive result is due to the increased flux from the spots overcoming the intrinsic weakening of the TiO band in warmer spots (in agreement with Paper II). The opposite is true for the 8860 Å band, where the f_S needed to fit increases with increasing T_S in this temperature range. In this band, the intrinsic strengthening of the band head in spotted regions overcomes the weaken-

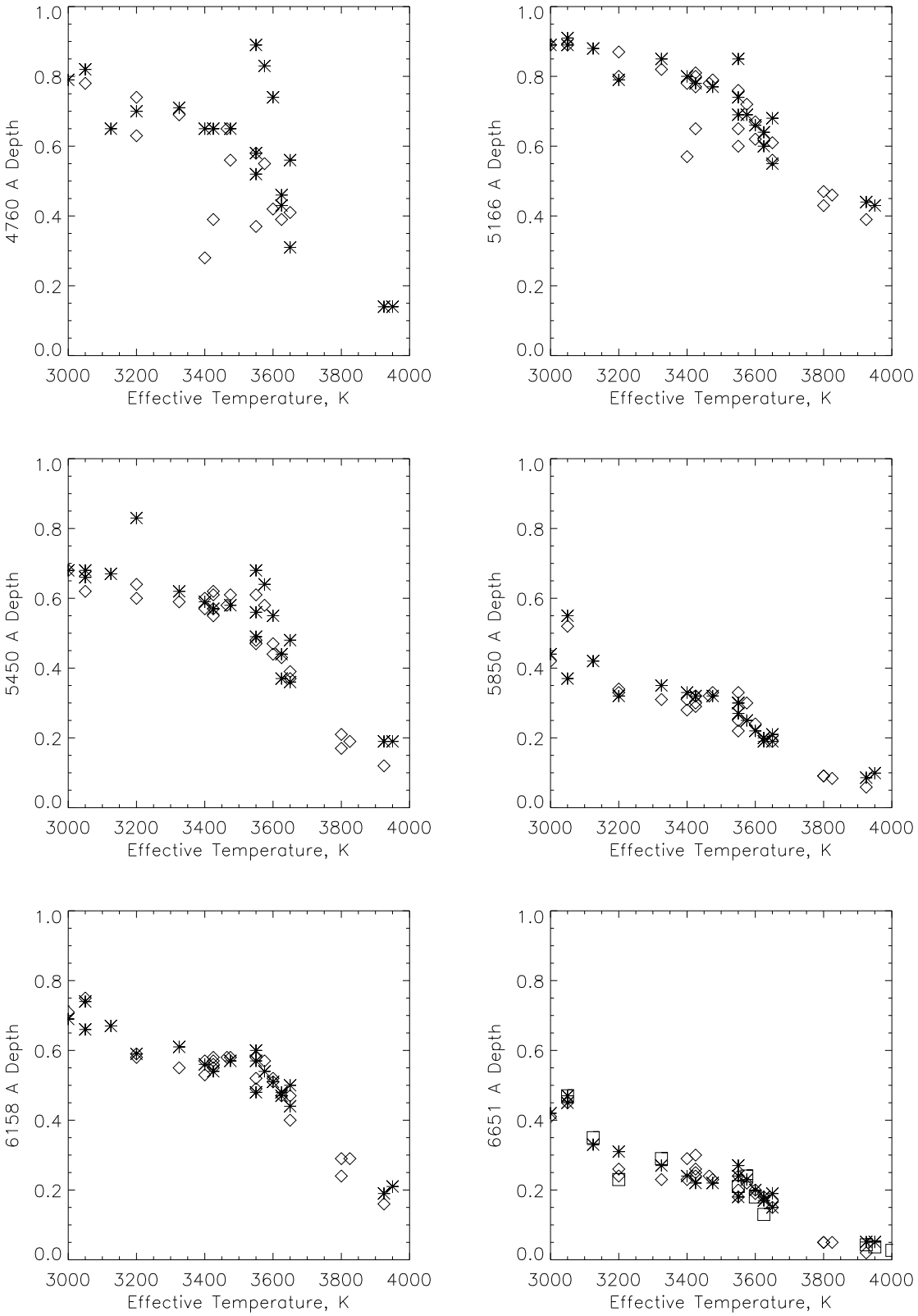

FIG. 1.—Plots of the depths of several molecular bands vs. $T_{\rm eff}$ for M giant comparison stars. A depth of 0 represents no band absorption, while a depth of 1 represents zero residual intensity inside the band. Asterisks represent measurements taken from FOE spectra of the comparison stars, diamonds represent QDSS spectra, and squares (for bands where $\lambda > 6500$ Å) represent Cassegrain Echelle spectra.

ing flux from cooler spots. The point at which the best-fitting f_S versus T_S relations for the two bands intersect determines f_S and T_S (§ 2.3); in this example, $T_S = 3570$ K and $f_S = 0.40$ (Fig. 3).

We then investigated how f_S needed to fit the 6650 and 6158 Å bands varies with T_S, and whether fitting these bands will further constrain the derived starspot parameters. In Figure 3, we see that in this T_S range, the f_S needed

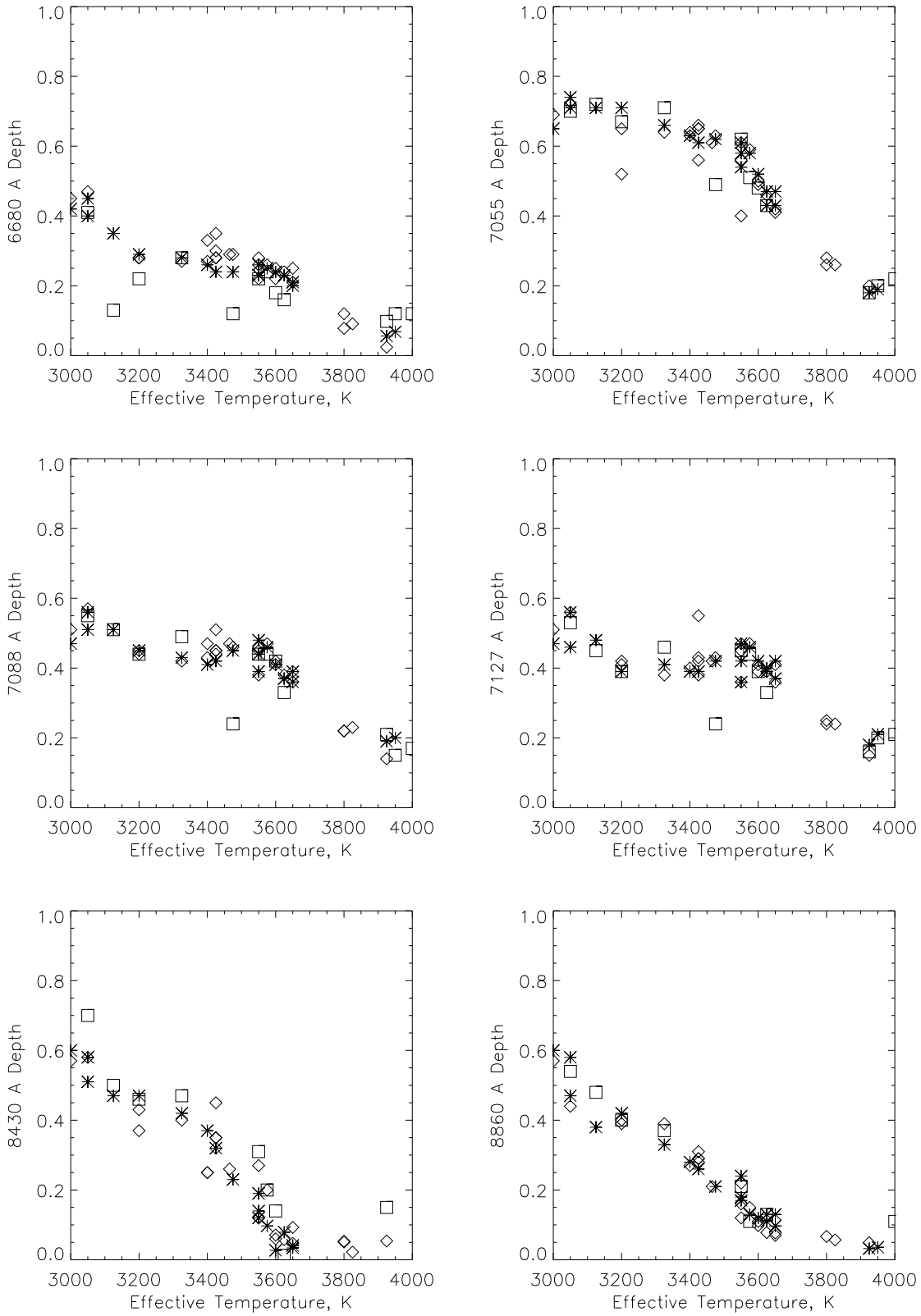

FIG. 1.—*Continued*

to fit a given band strength for these bands decreases with increasing temperature. The linear fit for the 6650 Å order is quite similar to that for 7055 Å, though less reliable, because of the relative weakness of the 6650 Å features. The linear fit for the 6158 Å band lies between 0.06 and 0.15 below those for both the 7055 and 6650 Å orders. Ideally, all four fits should intersect at a common point; the fact that the 6158 Å fit does not casts doubt on its usefulness for starspot studies. The difficulty is likely due to problems accurately normalizing the 6158 Å band and to its shorter wavelength, and

TABLE 4

MOLECULAR BANDS MEASURED IN M GIANT COMPARISON STARS

Wavelength (Å)	Molecule	Percent Depth at 3550 K[a]
4590	TiO	43
4630	TiO	41
4670	TiO	34
4760	TiO	58
4810	TiO	44
4845	MgH	30
4950	TiO	76
5010	TiO	36
5166	TiO	75
5450	TiO	61
5500	CaOH	26
5850	TiO	30
6158	TiO	58
6389	CaH	14
6651	TiO	24
6680	TiO	23
6713	TiO	27
6746	TiO	13
6920	CaH	17
7055	TiO	61
7088	TiO	45
7127	TiO	45
8430	TiO	19
8860	TiO	22

[a] Mean of measurements in FOE spectra of BY Boo.

thus smaller R_λ and lower sensitivity to spots. We did compute STARMOD fits to all the spectra of the active stars in all four orders where possible, but except where noted we use only fits to the 7055 and 8860 Å bands to derive f_S and T_S.

To choose the "best" values for f_S and T_S for II Peg in 1995 January (given in Table 2), we considered fits using four different nonspot comparison stars: κ Gem ($T_{\rm eff}$ = 4975 K), δ Boo ($T_{\rm eff}$ = 4900 K), HR 3808 ($T_{\rm eff}$ = 4750 K), and δ Cnc ($T_{\rm eff}$ = 4625 K). Ideally, we would use subgiant stars to fit spectra of II Peg; however, we were limited by the spectra available, and wherever possible we use comparison star data observed with the same instrumental set-up as the active star. In general we found that fits using nonspot comparison stars of similar $T_{\rm eff}$ but different gravities yield quite similar results.

To compute the uncertainties listed in Table 2, we collected the (T_S, f_S) values at which the fits for the 7055 and 8860 Å bands intersect for the various T_Q values used in fitting. The uncertainty for T_S is one-half the difference of the highest and lowest T_S values at which the two fits intersected. The f_S uncertainty was computed in the same way. The spectrum of January 20 (ϕ = 0.01) had insufficient S/N ($\sim$30; affected by clouds during the observation) at the 8860 Å band, so the f_S listed in Table 2 represents the value obtained from the 7055 Å band alone assuming T_S = 3550 K. The measured f_S values (for all FOE spectra of II Peg) are between 0.26 and 0.35, considerably lower than those measured using the band-depth technique for 1989 October and 1992 September (Paper II). The temperature T_S is slightly higher, $\approx$3530 $\pm$ 100 K, but not significantly so.

Between 1992 August and 1994 October we obtained 22 spectra of II Peg on 17 different nights with the QDSS Echelle Spectrograph at BMO. In these observations, the spectrograph was set up so that the 8860 Å TiO band head fell too close to the edge of the chip to be usable. We were able to fit only the 7055, 6650, and 6158 Å orders, and, given the similar behavior of the f_S versus T_S relations when those orders are fitted, we assumed T_S = 3530 K, as found from the FOE spectra. For nonspot comparison stars, we used spectra of six G/K dwarfs (since no G/K giants were observed during our BMO observing runs; experiments with FOE II Peg spectra showed that changing between giant and dwarf nonspot comparison stars made no significant difference in the derived parameters) covering 4575 K $\leq T_{\rm eff} \leq$ 5175 K, while for spot comparison stars we used M giant spectra with 3400 K $\leq T_{\rm eff} \leq$ 3650 K. The 7055 Å order was fitted over the wavelength range 6980–7130 Å; the intervals for the other orders were 6070–6190 Å and 6600–6800 Å.

For the BMO spectra, the f_S versus T_S relations obtained by fitting the 6650 and 6158 Å orders were again similar to those for the 7055 Å order. We thus derive f_S values using the 7055 Å order alone. Lacking data for the 8860 Å order introduces an uncertainty, given the possibility of a variable T_S (Byrne et al. 1995; O'Neal, Saar, & Neff 1998). The f_S listed in Table 2 for the BMO spectra are averages of f_S values obtained using nonspot comparison spectra with $T_{\rm eff}$ = 4850 and 4750 K. These typically differed by $<$0.05.

In Figure 4 we plot f_S for II Peg in 1992 as a function of phase. A wave is seen in the f_S values, with maximum spot coverage between phases 0.8 and 0. The phases of maximum and minimum f_S found from the BMO data agree with those calculated from the McMath-Pierce observations, while the BMO f_S values at each given phase are $\sim$0.06 less than those given in Paper II. About a third of this difference can be accounted for by our use in this study of T_S = 3530 K, 30 K warmer than the value used in Paper II. The remaining difference is within the experimental uncertainties of both techniques and might be due to factors such as the use of G and K dwarfs instead of giants to fit the BMO II Peg spectra and the lower resolution of the BMO data.

We then analyzed contemporaneous photometric data to see whether they were consistent with our TiO results. As in Paper II, we generated synthetic photometry by constructing model spectra from weighted sums of Kurucz models (with log g = 3.5) using equation (1), an assumed value of T_Q, and T_S and f_S derived from TiO bands. These model spectra were convolved with the appropriate filter response functions, and the results were compared with available photometry. Henry et al. (1995) present photometric spot models for II Peg covering 1973–1992, and G. Henry (1997, private communication) kindly provided the original photometric data used in that paper. During 1992 August–October, ($B-V$) varied from $\approx$1.015 to 1.035. Synthetic photometry based on our spot parameters (with T_S = 3530 K) gave the best fit to the ($B-V$) data when T_Q = 4750 K. With the same T_S, the McMath-Pierce f_S values also match the observed ($B-V$) best for T_Q = 4750 K. The V magnitude varied from $\approx$7.47 to 7.67 during this epoch. If the unspotted "immaculate" brightness of II Peg is $V(f_S$ = 0) = 6.8 (Paper II), then the f_S values found in our BMO data imply $\Delta V \approx 0.22$ and V magnitudes $\approx$0.2 mag too bright. Values of $f_S \approx 0.1$ greater are needed to match the observed V magnitude of II Peg. As in Papers I and II, this may be explained by our use here of M giant spectra as spot proxies for the subgiant star II Peg, which, given the increase of intrinsic TiO band depth with decreasing gravity (Paper I), would lead us to compute a smaller f_S than is

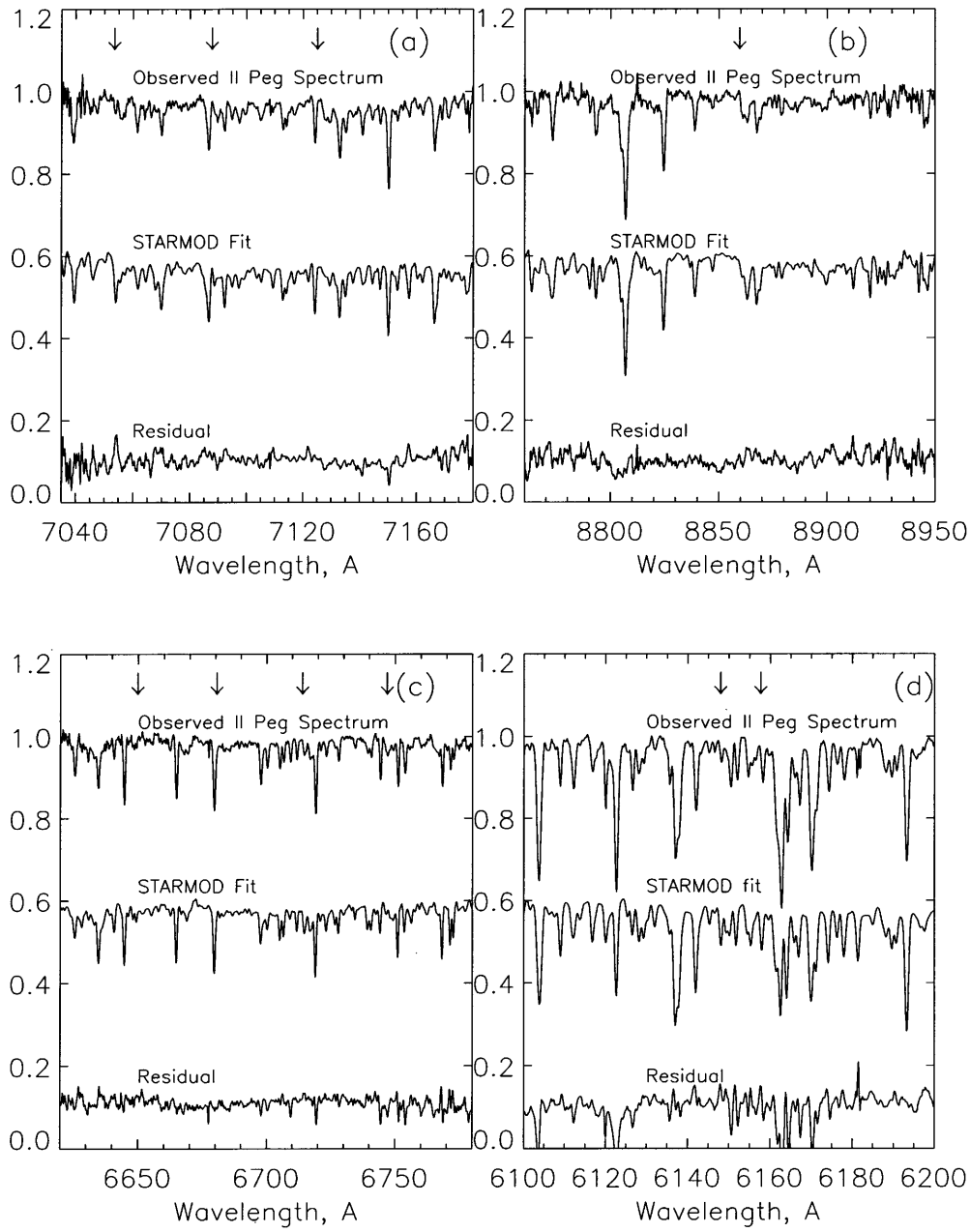

FIG. 2.—Best fits computed using STARMOD for the 7055, 8860, 6158, and 6650 Å absorption bands in the II Peg spectrum of 1995 January 19. Band head positions are shown with arrows. These fits use $T_Q = 4750$ K and $T_S = 3550$ K. Residuals are shown at the bottom of each plot, with 0.1 added for ease of illustration.

actually present. If the maximum f_S is closer to 0.6, the T_Q value that best fits the observed $(B-V)$ data increases to 4775 K.

We do not yet possess photometry contemporaneous with our 1995 January observations. However, Henry et al. (1995) list mean V magnitudes of II Peg for each of their data sets, covering a 19 yr span; the maximum was $\langle V \rangle = 7.4$. Our 1995 January observations have a mean f_S of 0.32. Taking $T_Q = 4750$ K, $T_S = 3530$ K, and $f_S = 0.32$ yields $\langle V \rangle = 7.18$, assuming $V(f_S = 0) = 6.8$. However, if we are underestimating f_S by ~ 0.1, $\langle V \rangle = 7.33$ for this epoch: brighter than the maximum $\langle V \rangle$ given by Henry et al. (1995) but not extremely so. We add the caveat that normalization was especially problematic for these data, since the 7055 Å band head fell close to the end of an order.

We analyzed two other echelle data sets for II Peg, both limited by incomplete coverage of the most useful TiO bands. During 1991 October 12–16, Huenemoerder (Byrne et al. 1995) obtained spectra of II Peg with the FOE at the Coudé Feed Telescope on Kitt Peak, which we have reanalyzed. This observing run used a smaller CCD (a 512 × 512 RCA), with the result that the 7055 and 7088 Å TiO band heads and the leading band of the 6650 Å system fell off the chip. For three of the five nights of this run, 32 spectra of II Peg were obtained each night; only two spectra were obtained on October 12 because of poor weather, and 20 spectra were obtained on October 13. In our reanalysis, we applied a median filter to sets of three consecutive II Peg spectra. Few observations of comparison stars were made during this run, so we used comparison stars from our later

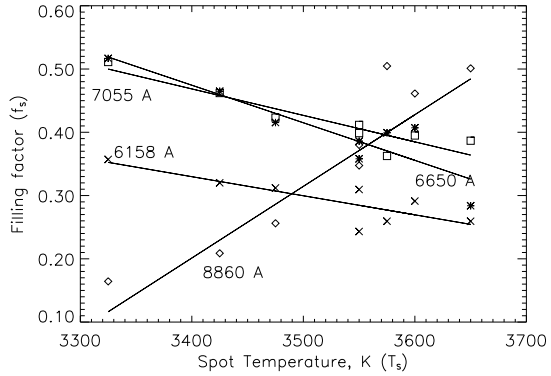

FIG. 3.—Values f_S vs. T_S computed with STARMOD for the II Peg spectrum of 1995 January 19, for each of the four molecular band regions modeled, together with best linear fits to each (6158 Å, *crosses*; 6650 Å, *asterisks*; 7055 Å , *squares*; and 8860 Å, *diamonds*), assuming $T_Q = 4750$ K. Unlike the other three bands, for the 8860 Å band, computed f_S increases with assumed T_S for 3325 K $\leq T_S \leq$ 3650 K. The values f_S and T_S for this spectrum are determined by the intersetion of the 8860 Å order fit with those of the 6650 and 7055 Å orders.

FOE data sets. We used eight M giant spot comparison stars spanning 3325 K $\leq T_{\rm eff} \leq$ 3650 K and five nonspot comparison stars spanning 4625 K $\leq T_{\rm eff} \leq$ 5000 K. STARMOD fits used 8820–8910 Å for the 8860 Å TiO band and 6680–6780 Å for the set of bands beginning at 6650 Å. For that order, although we lack the leading band head, we fitted those at 6710 and 6750 Å.

For these data we found $T_S = 3550 \pm 100$ K; $0.45 \leq f_S \leq 0.49$, with no coherent f_S variations detected within any one night. The similar results using the 6650 Å order indicate that they can be used as a substitute for the 7055 Å band. The approximately constant f_S for $\sim\frac{2}{3}$ of a rotation agrees with the photometry of Byrne et al. (1995). During this epoch, ΔV was $\approx$0.1 mag, and since $\langle V \rangle$ is similar to that seen in epochs with greater ΔV, a more uniform spot coverage is implied. The small variations in f_S that we compute for this epoch match the observed ΔV; $T_Q = 4750$ K provides the best match for the observed $(B-V)$. Once again, to match the observed V magnitudes [with $V(f_S = 0) = 6.8$], we need to invoke f_S values $\approx$0.06 higher than derived using TiO.

Finally, we obtained spectra of II Peg at two phases during 1995 December at McDonald Observatory. Poor weather affected the observations, and a cosmetic defect in the CCD near the 8860 Å band head renders the fits to this

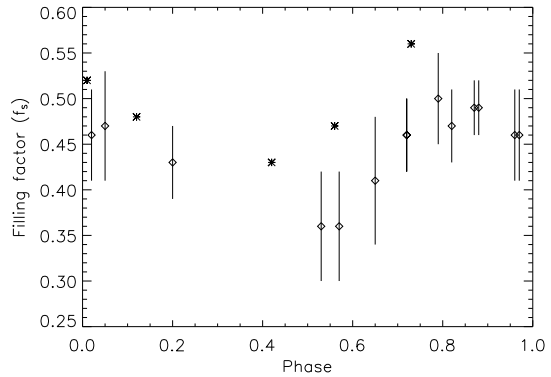

FIG. 4.—Computed f_S values for the II Peg spectra obtained with the QDSS during 1992 August–October. The asterisks represent McMath–Pierce observations from Paper II.

order unreliable. In these high-resolution ($R \approx 60{,}000$) spectra, the 6650 Å system of TiO was separated into two orders, the band heads at 6670 and 6710 Å fell into one order, and the leading 6650 Å band head appeared in the previous order. We fitted both these orders, plus the one containing the 7055 and 7088 Å TiO bands (the 7127 Å band head was not used). The spectral ranges fitted were 6665–6725, 6615–6670, and 7025–7090 Å. We used six M giant spot comparison spectra spanning 3325 K $\leq T_{\rm eff} \leq$ 3625 K and six G/K giant nonspot comparison spectra spanning 4625 K $\leq T_{\rm eff} \leq$ 5075 K. The higher spectral resolution did not alter the behavior of the f_S versus T_S relations. Assuming $T_S = 3550$ K and averaging the f_S values from fits using each of the nonspot comparison stars, we derive $f_S = 0.37 \pm 0.05$ for December 21 ($\phi = 0.58$) and $f_S = 0.40 \pm 0.05$ for December 26 ($\phi = 0.84$).

Our spectroscopic method for determining T_Q produced a poorly constrained result for II Peg. G and K giant stars with $T_{\rm eff} < 4600$ K clearly produced poorer fits to spectra of II Peg than did comparison stars with $T_{\rm eff} > 4600$ K, and there is a hint that nonspot comparison stars with $T_{\rm eff} \geq 5100$ K also fitted less well. This result is perhaps not surprising, since we are attempting to fit spectra of a subgiant active star with giant comparison spectra.

3.2. *EI Eri = HD 26337*

In Paper II we derived $T_S = 3700 \pm 200$ K and $T_Q = 5600$ K for this star and f_S between 0.15 and 0.38 in four epochs of observation. EI Eri is a single-lined G5 IV spectroscopic binary with $P_{\rm rot} = 1.95$ days, $v \sin i = 50$ km s^{-1}, and $\log g \approx 3.8$ (Paper II). We used the $\log g = 4.0$ Kurucz models to compute R_λ. We obtained seven FOE spectra of EI Eri in 1992 March, three in 1995 January, and two spectra at McDonald in 1995 December. Our T_Q fits indicate that cooler G and K giant comparison stars fitted EI Eri less well than warmer stars, but our nonspot grid did not extend high enough $T_{\rm eff}$ to derive T_Q.

Our warmest FOE G/K giant comparison star, 1 Gem, has $T_{\rm eff} = 5250$ K. To better match the suspected T_Q of EI Eri, we constructed an array of nonspot comparison stars using our three warmest G/K giant stars along with three G/K dwarf comparison stars, the warmest of which, κ^1 Cet, has $T_{\rm eff} = 5600$ K. For spot models we used eight M giant stars spanning 3550 K $\leq T_{\rm eff} \leq$ 3950 K. Because a gap exists in our FOE data set of M giant comparison stars between 3650 and 3925 K, we included two stars (36 Aql and α Vul) observed only at BMO in the spot comparison array for EI Eri. The lower resolution of the BMO spectra did not pose a problem in fitting the EI Eri spectra, because when the $R \approx 14{,}000$ FOE spectra are artificially broadened to match the $v \sin i = 50$ km s^{-1} of EI Eri, their effective resolution drops to the $R \approx 6000$ of the QDSS spectrograph. For each spectral order of interest, we fitted the same wavelength ranges as were used with II Peg.

When we fitted the 7055 Å order, we saw that the trend of decreasing f_S with increasing T_S does not continue for the entire T_S range. In Figure 5 we plot the f_S derived for each T_S value when the 7055 Å order of the 1992 March 24 EI Eri spectrum is fitted, using $T_Q = 5550$ K. For $T_S \gtrsim 3650$ K, the increased R_λ no longer overcomes the spot's intrinsically weaker TiO strength, and the relation reverses. The 6650 Å band behaves similarly. Figure 5 also shows fits to an II Peg spectrum using an unrealistically high T_S; a similar reversal is seen.

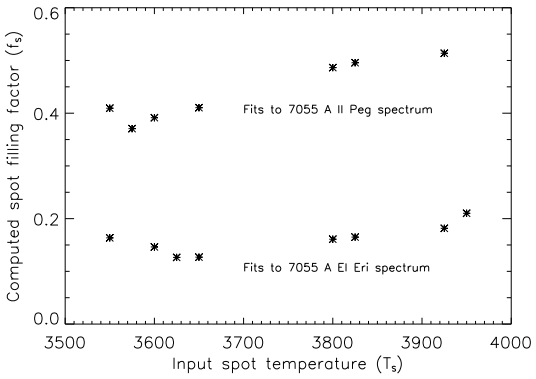

FIG. 5.—*Bottom*: Computed f_S vs. assumed T_S for the 7055 Å order in the 1992 March 24 spectrum of EI Eri. For $T_S \lesssim 3650$ K, f_S decreases with increasing T_S; the opposite behavior is observed for T_S higher than this. *Top*: Same turnover observed for the 7055 Å order in the 1992 October 14 BMO/QDSS spectrum of II Peg, when warmer spot comparison stars are used.

In many cases, the f_S values obtained from fitting the 8860 Å band in spectra of EI Eri did not overlap those for the 7055 Å order (both f_S (8860 Å) $> f_S$ (7055 Å) for all T_S, and the reverse, were seen). Presumably, the 8860 Å band is shallow enough to introduce substantial errors. However, fitting the 8860 Å order with $T_S \equiv 3650$ K returned nonzero f_S values, implying the band is present and thus that $T_S \lesssim 3800$ K.

EI Eri rotates in just under two days, so during a short observing run only two phases are visible. To determine f_S, we fitted the f_S versus T_S relations for the 7055 Å order with a second-order polynomial and read the f_S at $T_S = 3700$ K (the value from Paper II), averaged for the two warmest nonspot comparison stars ($T_{\rm eff} = 5600$ and 5550 K). No substantive difference between f_S on the two hemispheres was seen in the 1992 March data; $f_S = 0.30 \pm 0.08$ for all spectra. In contrast, the 1995 January data show one hemisphere to be essentially spot-free (January 18), while the other hemisphere (January 19 and 21) showed $f_S = 0.18 \pm 0.07$.

To fit our two McDonald spectra of EI Eri, we used a spot comparison array with $T_{\rm eff}$ values identical to those used for the FOE spectra. The nonspot comparison array differed in that we observed G giants of $T_{\rm eff} = 5650$ and 5400 K; we also used our two warmest G dwarf comparison stars. The 8860 Å order in these EI Eri spectra had insufficient S/N ($\lesssim$30) to produce reliable fits. The two observations were four days apart, meaning that approximately the same hemisphere was observed; we found $f_S = 0.15 \pm 0.06$.

3.3. *V1762 Cygni = HR 7275 = HD 179094*

Based on one pair of McMath-Pierce spectra and contemporaneous photometry, in Paper II we derived $T_S = 3450$ K and $T_Q = 4550$ K for V1762 Cyg. A K2 III–IV + G8V RS CVn binary (Osten & Saar 1998), V1762 Cyg has a 27.9 day period. Schrijver & Zwaan (1991) estimate $M/M_\odot \approx 2$ and Osten & Saar (1998) find $R/R_\odot \approx 6.4$, so $\log g \approx 3.1$; we used Kurucz models with $\log g = 3.0$ to fit this star.

We obtained seven spectra of V1762 Cyg at BMO. In 1993, the spectrograph was aligned so that the 8860 Å band head fell too close to the end of an order to be usable. In 1994 a larger CCD was in place, allowing the 8860 Å band to be observed, but not the 6650 Å bands. Most of our BMO comparison star spectra were obtained with the original set-up and thus lack the 8860 Å order. To fit the 1993 spectra we used an array of five G/K dwarf stars of 4325 K $\leq T_{\rm eff} \leq$ 4850 K, and nine M giant comparison stars with 3325 K $\leq T_{\rm eff} \leq$ 3800 K. To fit the 1994 spectra, we used FOE spectra of the same comparison stars where possible, artificially degrading the resolution to match that of the QDSS observations. No FOE spectrum of the $T_{\rm eff} = 4325$ K dwarf (61 Cyg A) was available. For the 8860 Å order, we fitted the wavelength range 8800–8900 Å.

In Table 2 we list the f_S values found for V1762 Cyg. For the 1993 spectra, we used the two coolest K giants ($T_{\rm eff} =$ 4325 K and 4575 K) as photospheric proxies, and took the f_S value at $T_S = 3450$ K in the best fit to the f_S versus T_S relations. Fitting the 1994 spectra including the 8860 Å order yielded $T_S = 3500 \pm 150$ K and the f_S values listed in Table 2, assuming $T_Q = 4575$ K. When warmer G/K dwarfs ($T_{\rm eff} \geq 4750$ K) were used as nonspot comparison stars, higher f_S values, in some cases approaching 0.35, were obtained. This is a result of the disappearance of the 7055 Å band seen in the cooler K dwarfs (Paper II). Our fits to the "band-free" spectral order yielded $T_Q = 4600 \pm 150$ K; comparison stars warmer or cooler fitted the order much more poorly than stars in this $T_{\rm eff}$ range.

3.4. *V1794 Cyg = HD 199178*

We obtained two spectra of V1794 Cyg with the FOE in 1992 March and three spectra with the QDSS in 1993–1994. V1794 Cyg is an FK Comae variable, a rapidly rotating ($v \sin i = 80$ km s^{-1}) single star that might be a coalesced binary (Huenemoerder 1986). Its light curve can change on timescales less than a month (Rodonò & Cutispoto 1992), and $P_{\rm rot} = 3.337$ days. The star's G5 III-IV spectral type implies $\log g \approx 3.3$; we use the Kurucz models for $\log g = 3.5$ to compute R_λ. In Paper II we found $0.16 \leq f_S \leq 0.37$ in two epochs of observation, $T_Q = 5350$ K, and $T_S = 3800$ K. We were unable to determine T_Q spectroscopically, since $T_Q > T_{\rm eff}$ of our warmest comparison stars.

Given the warmer spots on this star, the TiO bands alone cannot constrain T_S. We used the same spot comparison array as we did for EI Eri. We then fitted a second-order polynomial to the f_S versus T_S relations for each T_Q in order to determine f_S from the 7055 Å order fits at $T_S = 3800$ K. Using the 5250 K giant nonspot comparison star (1 Gem), we find $f_S = 0.20$ and 0.22 for spectra obtained on two consecutive nights in 1992 March. For the BMO spectra, using G dwarf nonspot comparison stars and averaging f_S values obtained for 5175 K $\leq T_Q \leq$ 5550 K, we find $f_S = 0.29 \pm 0.04$ for 1993 September 1 and 0.28 ± 0.04 for 1994 June 11. Two weeks later, observing nearly the opposite stellar hemisphere, $f_S \approx 0$.

3.5. *σ Geminorum = HD 62044*

We obtained fourteen spectra of σ Gem with the FOE (nine in 1992 March and five in 1995 January) and four with the Cassegrain Echelle at McDonald. σ Gem is a single-lined spectroscopic binary with a K1 III spectral type, a 19.4 day period, and $v \sin i = 25$ km s^{-1}. From tables in Gray (1988), we estimate $\log g \approx 2.5$. In Paper II we found $T_Q = 4500$ K, $T_S = 3850$ K, and f_S ranging from 0 to 0.33 during seven epochs of observation.

To fit the FOE spectral orders, we used spectra of eight G/K giant comparison stars with 4200 K $\leq T_{\rm eff} \leq$ 4900 K

and six M giant stars with $3550 \leq T_{\rm eff} \leq 3950$ K. Since the 8860 Å band depth is negligible, $T_S \geq 3800$ K. We used spectra of the same comparison stars to fit the McDonald spectra of σ Gem. Using the warmer nonspot comparison stars produced substantially higher f_S values, since the small contribution to the 7055 Å band depth from the nonspot photosphere disappears for $T_Q \gtrsim 4700$ K.

In Table 2 we list the f_S values derived for σ Gem. Our 1992 March observations spanned nearly half of a rotation period, and we found roughly uniform spot coverage. In 1995 January, an area of greater spot coverage was appearing on the final two nights of observation. In our McDonald spectra, the first two observations, $\phi = 0.11$ and 0.16, showed about half as much spot coverage as the latter two, $\phi = 0.36$ and 0.41.

Henry et al. (1995) provide photometry contemporaneous with our 1992 March observations. Variations in V at that epoch were between $V = 4.23$ and $V = 4.30$; $(B-V)$ was between 1.11 and 1.12. These variations were matched to within 0.01 mag using our computed f_S values along with $V(f_S = 0) = 4.14$ (Paper II), $T_S = 3850$ K, and $T_Q = 4500$ K. The higher f_S values derived for $T_Q \gtrsim 4700$ K do not yield good fits to contemporaneous photometry. The good match between photometry predicted from our f_S values and observed photometry, in contrast to the case for II Peg, is likely due to the fact that σ Gem is a giant star and M giants are better proxies for its spots than for the spots on II Peg.

σ Gem, as a giant star, yielded the best results of any of our target stars when we fitted the "band-free" spectral order to determine T_Q (Fig. 6). Using the rms values produced from fitting a full FOE spectral order of σ Gem, we find $T_Q = 4600 \pm 200$ K.

3.6. *DM Ursae Majoris*

This star has a 7.49 day period and $v \sin i = 26$ km s^{-1}; the spectral type is K2 III–IV (Charles, Walter, & Bowyer 1979) or K0-1 III–IV (Kimble, Kahn, & Bowyer 1981). From photometry, Kimble et al. (1981) found a total starspot coverage on the star of at least 16% and perhaps as much as 33%, depending upon the inclination, and $T_S \approx$ 700–1300 K cooler than the photosphere. Mohin & Raveendran (1992) find $T_S = 3400 \pm 60$ K and $T_Q = 4750$ K. Hatzes (1995a) derives $T_Q = 4500$ K and $T_S = 3300$ K from his Doppler imaging.

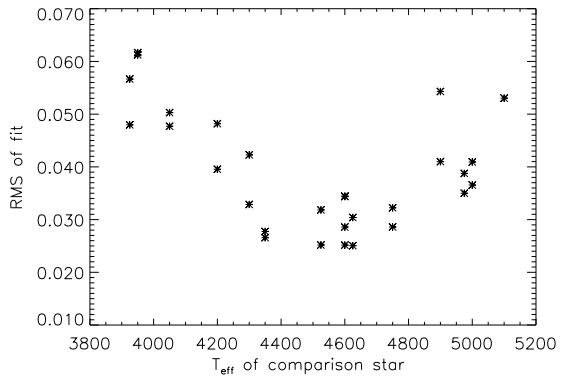

FIG. 6.—Illustration of the method by which we constrain T_Q spectroscopically. The value $T_{\rm eff}$ for the G and K giant nonspot comparison stars is plotted against the rms obtained when we use each spectrum to fit the 6240–6410 Å order of the σ Gem spectrum of 1995 January 19. Comparison spectra with $T_{\rm eff} = 4600 \pm 200$ K clearly fitted the σ Gem spectrum better; thus we conclude that T_Q for σ Gem is in this range.

We obtained two spectra of DM UMa with the FOE and one at McDonald. Since these were our first observations of this star, we used a complete temperature range of spot comparison stars, $3050 \text{ K} \leq T_{\rm eff} \leq 3950$ K. We used G/K giants with $4325 \text{ K} \leq T_{\rm eff} \leq 5000$ K as nonspot comparison stars. By fitting the 7055 and 8860 Å orders in the FOE spectra, we derived $T_S = 3570 \pm 100$ K and $f_S = 0.30 \pm 0.10$ for 1995 January 19, and 0.35 ± 0.08 for January 22 (assuming $T_Q = 4500$ K). In the McDonald spectrum, the 8860 Å order was too weak to be used, but fitting the 7055 Å order yielded $f_S \approx 0.25$ if $T_S = 3600$ K is assumed. By fitting the "band-free" order we derived $T_Q \geq 4600$ K.

3.7. *HU Virginis = HD 106225*

This star has $v \sin i = 25$ km s^{-1} (Fekel, Moffett, & Henry 1986) and $P_{\rm rot} = 10.4$ days. Strassmeier (1994) finds a large polar spot with a total area coverage of $\approx$10% of the star and $\Delta T = 1000$–1500 K. He also derives $\log g \approx 3.0$ and $T_Q = 5000$ K.

We obtained only one spectrum of this star, on 1995 January 23 with the FOE. Our fits imply cooler spots covering a larger area: $T_S = 3440 \pm 100$ K and $f_S = 0.44 \pm 0.06$ (assuming $T_Q = 5000$ K). More observations are needed to confirm this result. Spectroscopically, we derived $T_Q = 5000 \pm 150$ K, although this is not a firm result because of the small number of comparison stars warmer than this, and because HU Vir is a subgiant.

3.8. *λ Andromedae = HR 8961 = HD 222107*

This star is a nonsynchronous rotator, with $P_{\rm rot} = 54.05$ days and $P_{\rm orb} = 20.5$ days. The visible component of this single-lined binary is a G8 III–IV star with $T_{\rm eff} = 4750 \pm 30$ K, $v \sin i = 6.5$ km s^{-1}, and $\log g = 2.5$ (Donati, Henry, & Hall 1995).

Donati et al. (1995) derived a two-spot model for λ And with $T_S = 4000 \pm 300$ K, with the larger spot covering 8% of the photosphere. Their $V_{\rm max}$ was fainter than the historical light maximum of $V = 3.70$ (Boyd et al. 1983), indicating an additional 12% polar or uniform spot coverage. Henry et al. (1995) tracked 11 spots on λ And in 17 yr of photometry and find a long-term variation in maximum brightness of 0.13 mag, ΔV between 0.08 and 0.22 mag, and $\Delta T = 800$–1000 K.

We obtained three spectra of λ And in 1995 January with the FOE and two spectra at BMO in 1993. We used spot comparison stars spanning our entire $T_{\rm eff}$ range, and we use nonspot comparison stars with $4525 \text{ K} \leq T_{\rm eff} \leq 5250$ K. Table 2 lists our derived f_S values assuming $T_Q = 4750$ K. In 1995 January we found f_S as high as 0.23, but in late summer 1993 they were lower; in one BMO observation only an upper limit was obtained. For the FOE spectra, fitting of the 7055, 8860, and 6650 Å orders favored $T_S = 3650 \pm 150$ K. Our T_Q measurements did not yield a clear result, favoring $T_Q \geq 4650$ K.

3.9. *Emission-Line Strengths*

Echelle spectroscopy permits the simultaneous monitoring of chromospheric emission features and molecular bands. Many (though not all) studies have found positive correlations between emission-line strengths and starspot coverages in active stars (e.g., Dempsey et al. 1993b; Hatzes 1995a). Qualitatively, this is expected if the starspots and plage regions are spatially coincident. Following Barden

(1985), we use the equivalent widths of the emission features to activity levels. For each active star, we chose at least one comparison star of a similar $T_{\rm eff}$ and luminosity class, whose spectrum was rotationally broadened and coaligned with the active star spectrum. Subtracting the modified comparison spectrum from the active star reveals any excess emission. For the FOE spectra, the Ca II H and K lines, Hα, and two of the three infrared triplet lines (8498 and 8542 Å) fell on the CCD. In the McDonald spectra and the BMO spectra taken with the RCA chip, Hα and all three Ca II IRT lines were obtained, except in 1994 at BMO, when the 8542 and 8663 Å lines were not observed.

The spectral-subtraction procedure is illustrated in Figure 7 for the orders of the 1995 January 19 spectrum of II Peg containing Hα and the Ca II IRT. The most redward line of the infrared triplet, 8663 Å, was not observed in this epoch. The comparison star is HR 3808, $T_{\rm eff} = 4750$ K. After the comparison spectrum is rotationally broadened, it matches the spectrum of II Peg quite well, except in the chromospheric emission lines of interest.

II Peg, DM UMa, and HU Vir are the three active stars in this study, with emission reversals in Hα and the infrared triplet in their raw (unsubtracted) spectra. For the other stars, emission (line core filling) in these lines is only evident in the subtracted spectra. We define W_λ as the emission equivalent width in the raw spectrum and W'_λ as the emission equivalent width after spectral subtraction. In Table 5 we list the comparison stars used in spectral subtraction for each active star. In the case of II Peg, different comparison stars were used for the different data sets, determined by the availability of high S/N spectra of the various standards. In Table 6 we present W'_λ values for Hα, the Ca II IRT, and Ca II H and K for our active star spectra.

Dempsey et al. (1993a) found anticorrelations between Ca II IRT emission strengths and stellar brightness for several active stars. Weak correlations between spot and chromospheric activity were found for II Peg by Andrews et al. (1988) and Rodonò et al. (1986), while none was found for the active dwarf star AU Mic by Butler et al. (1987). Figure 8 is a plot of f_S against W'_λ for the infrared triplet and Hα for our 1992 BMO spectra of II Peg (showing the densest phase coverage in our data set). Excluding the one anomalously high emission point (a possible flare seen in all three IRT lines and Hα), we find a strong correlation between f_S and W'_{8498}, with a correlation coefficient of 0.82, giving a 4% probability that the two data sets are inherently uncorrelated. The correlation is weaker (19% probability of

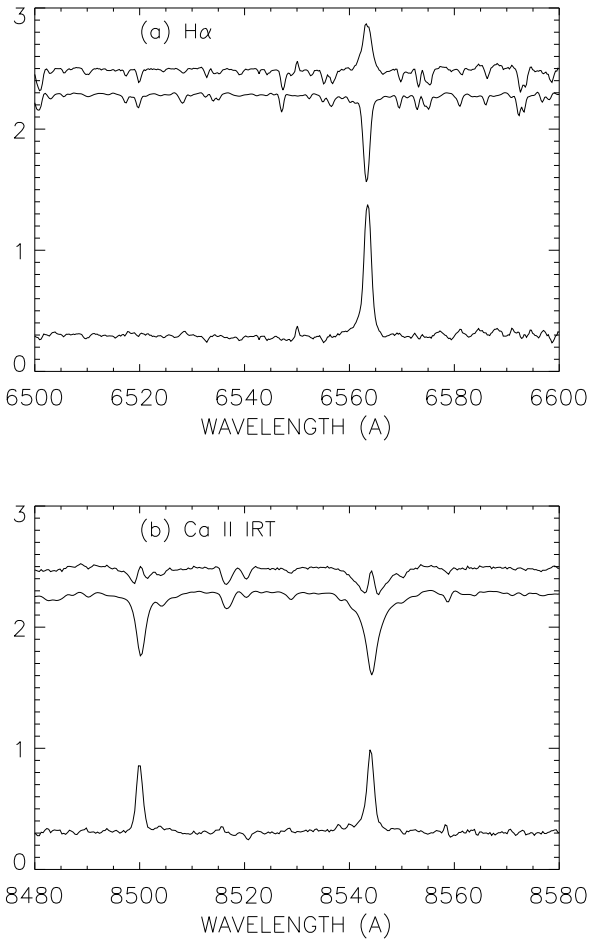

FIG. 7.—(*a*) Order containing Hα in the 1995 January 21 spectrum of II Peg taken with the FOE (*top*). Immediately below the II Peg spectrum is a rotationally broadened spectrum of δ Boo, and at bottom is the difference between the two spectra, illustrating the excess emission in the spectrum of II Peg. (*b*) Similar plot illustrating two of the lines in the Ca II infrared triplet observed in the same spectrum.

TABLE 5

COMPARISON STARS USED FOR EMISSION-LINE MEASUREMENTS

Active Star	Data Set	Comparison Star(s)	Spectral Type	$T_{\rm eff}$
II Peg	1991 Oct	δ Boo	G8 III	4900
	1992-94 BMO	Gl 688	K3 V	4850
	1995 Jan	δ Boo	G8 III	4900
	1995 Dec	HR 3808	K0 IV	4750
EI Eri	1992 Mar	1 Gem	G5 III–IV	5250
	1995 Jan	1 Gem	G5 III–IV	5250
	1995 Dec	β Pyx	G4 III	5400
V1762 Cyg.....	1993–1994 BMO	χ Gem	K2 III	4525
V1794 Cyg.....	1992 Mar	1 Gem	G5 III–IV	5250
	1993–1994 BMO	1 Gem	G5 III–IV	5250
σ Gem	1992 Mar	χ Gem	K2 III	4525
	1995 Jan	χ Gem	K2 III	4525
	1995 Dec	χ Gem	K2 III	4525
DM UMa	1995 Jan	58 Leo	K1 III	4600
	1995 Dec	σ Hya	K1 III	4600
HU Vir	1995 Jan	HR 3808	K0 IV	4750
λ And	1993 BMO	κ Gem	G8 III	4975
	1995 Jan	κ Gem	G8 III	4975

TABLE 6

EMISSION STRENGTHS FROM ACTIVE STARS

Star	Date (UT)	H	K	W'_λ (Å) Hα	8498 Å	8542 Å	8663 Å
II Peg	1991 Oct 12	…	…	…	0.99	1.11	…
	1991 Oct 13	…	…	…	0.91	1.14	…
	1991 Oct 14	…	…	…	0.89	1.13	…
	1991 Oct 15	…	…	…	0.83	1.06	…
	1991 Oct 16	…	…	…	0.96	1.20	…
	1992 Aug 2	…	…	2.12	0.99	2.36	1.36
	1992 Aug 3	…	…	1.52	0.93	2.06	1.23
	1992 Aug 6	…	…	1.73	0.91	1.87	1.19
	1992 Aug 7	…	…	2.17	1.12	1.89	1.34
	1992 Aug 12	…	…	1.83	0.83	1.79	1.17
	1992 Aug 19	…	…	2.08	1.18	2.06	1.31
	1992 Aug 20	…	…	1.76	0.89	1.95	1.18
	1992 Aug 22	…	…	3.47	1.47	2.95	1.81
	1992 Oct 14	…	…	1.81	0.98	2.27	1.21
	1992 Oct 27	…	…	2.57	1.03	2.25	1.38
	1992 Oct 28	…	…	2.26	1.01	2.24	1.36
	1993 Aug 22	…	…	2.65	1.01	2.32	1.46
	1993 Sep 12	…	…	2.10	1.08	1.64	…
	1993 Sep 14	…	…	3.33	0.64	1.56	1.55
	1993 Dec 17	…	…	1.67	0.58	…	1.10
	1994 Oct 4	…	…	2.25	0.45	…	…
	1994 Oct 6	…	…	2.06	0.43	…	…
	1995 Jan 19	1.24	0.96	2.22	0.88	1.16	…
	1995 Jan 20	0.70	0.79	2.00	0.92	1.18	…
	1995 Jan 21	2.21	1.29	2.08	0.94	1.19	…
	1995 Jan 23	2.17	1.23	1.92	0.94	1.30	…
	1995 Dec 21	…	…	1.86	…	…	…
	1995 Dec 26	…	…	2.06	1.04	1.42	0.97
EI Eri	1992 Mar 19	1.85	0.96	0.68	0.65	1.42	…
	1992 Mar 20	1.37	1.09	0.80	0.62	1.31	…
	1992 Mar 21	2.66	0.82	0.75	0.69	1.51	…
	1992 Mar 23	1.95	1.07	0.76	0.71	1.38	…
	1992 Mar 24	2.48	0.98	0.87	0.71	1.47	…
	1992 Mar 25	1.92	1.01	0.79	0.58	1.28	…
	1992 Mar 26	2.43	0.90	0.50	0.69	1.50	…
	1995 Jan 18	…	0.90	0.61	0.72	1.33	…
	1995 Jan 19	2.35	1.84	0.75	0.57	1.25	…
	1995 Jan 21	2.99	2.23	0.80	0.60	1.03	…
	1995 Jan 23	2.44	2.17	0.76	0.64	1.13	…
	1995 Dec 21	…	…	0.76	…	…	…
	1995 Dec 25	…	…	0.70	0.77	0.96	0.97
V1762 Cyg	1993 Aug 19	…	…	0.32	0.53	0.42	0.24[a]
	1993 Sep 14	…	…	0.33	0.76	0.83	0.69
	1994 Jun 11	…	…	0.22	0.26	…	…
	1994 Jul 2	…	…	0.24	0.45	0.58	…
	1994 Jul 17	…	…	0.29	0.53	0.73	…
V1794 Cyg	1992 Mar 24	1.30	1.34	0.82	0.62	1.03	…
	1992 Mar 25	1.22	0.98	0.57	0.57	0.97	…
	1993 Sep 11	…	…	0.41	0.71	1.73	…
	1994 Jun 11	…	…	0.39	0.50	…	…
	1994 Jul 2	…	…	0.80	0.29	…	…
σ Gem	1992 Mar 17	0.77	0.88	0.16	0.44	0.71	…
	1992 Mar 19	0.77	0.90	0.15	0.42	0.54	…
	1992 Mar 20	1.00	0.71	0.15	0.38	0.58	…
	1992 Mar 21	0.97	0.71	0.22	0.42	0.60	…
	1992 Mar 22	1.05	0.69	0.17	0.52	0.69	…
	1992 Mar 23	0.81	0.72	0.20	0.45	0.52	…
	1992 Mar 24	0.97	0.72	0.17	0.48	0.65	…
	1992 Mar 25	0.64	0.71	0.17	0.42	0.49	…
	1992 Mar 26	0.79	0.67	0.16	0.45	0.52	…
	1995 Jan 18	0.91	0.66	0.10	0.27	0.43	…
	1995 Jan 19	1.07	0.71	0.18	0.28	0.46	…
	1995 Jan 21	1.38	0.70	0.15	0.23	0.32	…
	1995 Jan 22	1.01	0.78	0.16	0.27	0.34	…
	1995 Jan 23	1.26	0.75	0.18	0.26	0.28	…
	1995 Dec 20	…	…	0.15	0.37	…	…
	1995 Dec 21	…	…	0.15	0.33	…	…
	1995 Dec 25	…	…	0.13	0.27	…	…
	1995 Dec 26	…	…	0.21	0.31	…	…

TABLE 6—*Continued*

Star	Date (UT)	H	K	W'_λ (Å) Hα	8498 Å	8542 Å	8663 Å
DM UMa	1995 Jan 19	2.76	1.34	4.15	0.97	1.72	...
	1995 Jan 20	1.99	1.47	2.52	0.98	1.55	...
	1995 Jan 23	1.66	1.26	2.15	0.93	1.62	...
	1995 Dec 26	...	...	1.81	0.73	1.22	0.89
HU Vir	1995 Jan 23	1.55	1.05	1.52	0.91	1.09	...
λ And	1993 Aug 22	...	...	0.53	0.85	1.42	0.42[b]
	1993 Sep 14	...	...	0.28	0.65	0.95	0.16
	1995 Jan 19	1.07	0.88	0.35	0.49	1.02	...
	1995 Jan 20	1.08	0.78	0.33	0.55	0.84	...
	1995 Jan 23	1.17	0.85	0.47	0.44	0.82	...

[a] Since the 8863 Å line did not fall on the chip for the comparison star spectrum used, these measurements use the star Gl 570A, K4 V, $T_{\rm eff} = 4575$ K as a standard.

[b] Since the 8863 Å line did not fall on the chip for the comparison star spectrum used, these measurements use the star Gl 688, K3 V, $T_{\rm eff} = 4850$ K as a standard.

inherent noncorrelation) between f_S and W'_{8542}. In Figure 8, the strengths of the 8663 Å line and Hα appear nearly constant with f_S, although there is still a slight positive correlation. No correlations between emission strength and f_S were found in the smaller 1995 January FOE data set.

For other stars, the two FOE data sets of EI Eri show a possible correlation between f_S and Ca II H and K emission; $r = 0.76$, yielding an 11% probability of inherent noncorrelation. Ca II IRT variations disagree with Ca II HK, however, while Hα is approximately constant. Thus, correlations between f_S and W'_λ for EI Eri are inconsistent and inconclusive. For σ Gem we possess almost nightly observations from both FOE runs, but no convincing correlations were found between f_S and emission strengths.

The lack of consistent correlation between f_S and emission strength confirms previous indications that starspots are sometimes, but not always, spatially coincident with regions of enhanced activity. One possible explanation comes from solar observations, where observations show that chromospheric emission is actually much lower over umbrae and over surrounding plage and active network. Sams, Golub, & Weiss (1992), discussing a similar phenomenon seen in X-rays, suggest that magnetic wave heating above sunspots may be suppressed due to the inhibition of

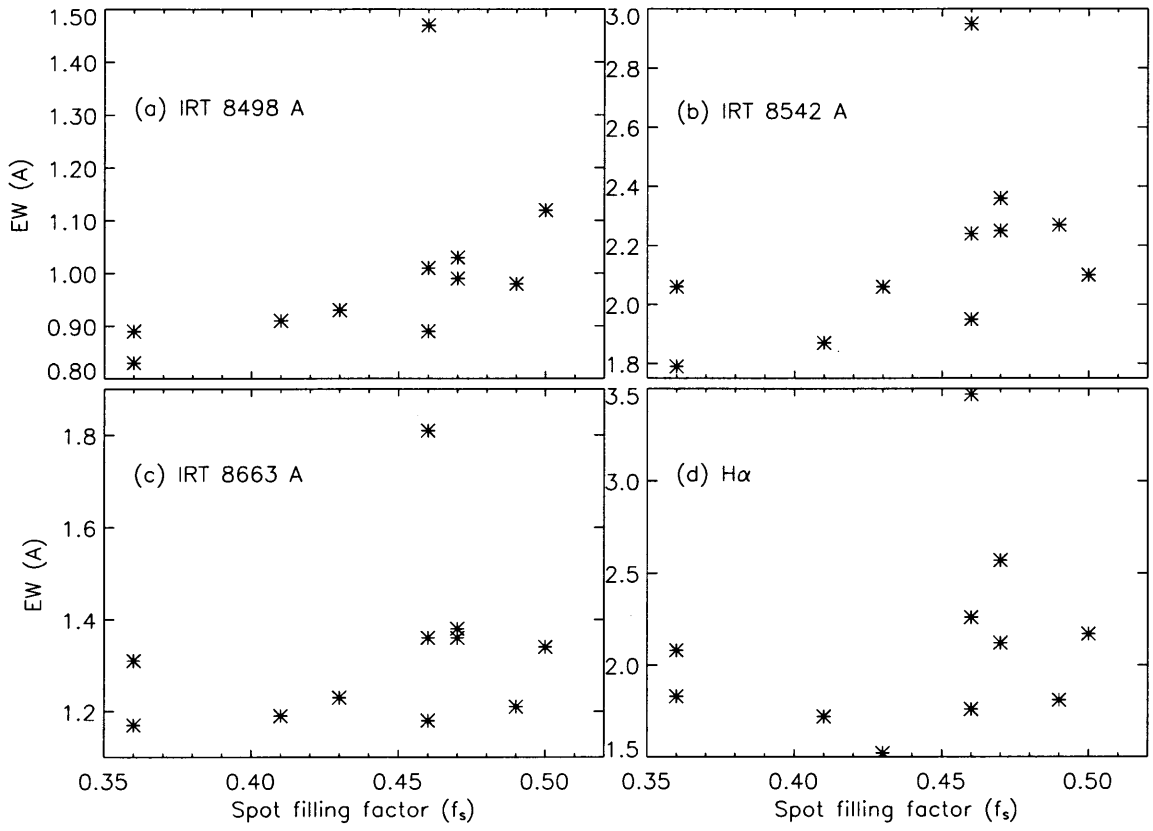

FIG. 8.—Plots of spot-filling factor vs. the emission strength (W'_λ) of the three infrared triplet lines and of Hα for the II Peg spectra of 1992 August–October taken with the QDSS. The Ca II 8498 and 8542 Å lines yield the best evidence in this study for a correlation between emission strength and spot-filling factor. The correlation is less apparent with Hα and the Ca II 8498 Å line.

flux tube footpoint "shaking" by the strong umbral magnetic fields. Thus, if starspots are truly the stellar analog of sunspot umbrae, they may be areas of somewhat *reduced* chromospheric emission (at least compared to nearby plage/network). In addition, strong plage could occur at regions of the star's surface far from the spot coverage. The relative amount of plage and spot visible at a given time and the degree to which the spot field suppresses flux tube motion on a given star may therefore lead to quite complex and variable relationships between f_S and emission.

4. DISCUSSION

4.1. *Relations Between T_S and Computed f_S Values*

The sharply different behavior of the 8860 Å band and the 7055 Å band (or most any other TiO feature we have studied) is important for simultaneously constraining f_S and T_S (e.g., Fig. 5). When we extended the $T_{\rm eff}$ range of M giant comparison stars, we found that the relation between computed f_S and assumed T_S "turns over" at $T_S \approx 3650$ K for the 7055 Å band, with higher T_S requiring progressively larger f_S values to match the feature. The 8860 Å band shows a change at low $T_{\rm eff}$; the relation between computed f_S and assumed T_S appears to turn over near 3200 K.

To investigate these f_S versus assumed T_S relations in more detail, we computed them using the depth versus $T_{\rm eff}$ relations for M giant comparison stars from Paper II and assuming band-depth and T_Q values for a hypothetical active star. From equation (1) we can derive

$$f_S = \frac{D_{\rm ac}}{D_{\rm ac} - R_\lambda[1 - D_S - (1 - D_{\rm ac})^{-1}]}, \qquad (3)$$

where f_S is the spot-filling factor and D_S and $D_{\rm ac}$ are the depths of the molecular band in the spot comparison star ($T_{\rm eff} = T_S$) and the active star, respectively.

Figure 9 shows the results, assuming $D_{\rm ac} = 0.04$ for the 7055 Å band, $D_{\rm ac} = 0.03$ for the 8860 Å band, log $g = 3.5$ to compute R_λ, and $T_Q = 4800$ K. The curve for the 7055 Å band reproduces the observed turnover at $\approx$3650 K, and the 8860 Å curve appears to reach a minimum near $\approx$3200 K. (the kink at $\approx$3575 K, as discussed in Paper II, may be due to either a sharp change in band depth or a flaw in our

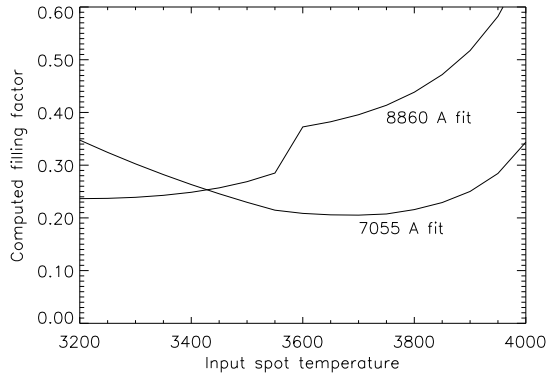

FIG. 9.—Values f_S vs. T_S computed with $T_Q \equiv 4800$ K for the 7055 and 8860 Å TiO bands of a hypothetical active star using a band-depth method similar to Paper II (see text), and the depth vs. $T_{\rm eff}$ relations for M giant spot comparison stars given in Paper II. We assume a 4% depth for the 7055 Å band and a 3% depth for the 8860 Å band in the active star. This calculation reproduces the turnover in the f_S vs. T_S relation for the 7055 Å band near $T_{\rm eff} = 3650$ K that was found by fitting the entire spectral order using STARMOD. It also reproduces the flattening of the f_S vs. T_S relation for the 8860 Å order at low T_S values.

$T_{\rm eff}$ scale around M3 III and M4 III). The similarity of Figure 9 to the T_S versus f_S relations derived by fitting the entire spectral orders is further evidence that the band-depth and STARMOD order-fitting methods for determining starspot parameters yield similar results. The shapes of the curves in Figure 9 are independent of $D_{\rm ac}$ and T_Q; they merely shift up or down when these parameters are changed. The similarity of the slopes of the relations for $T_S \gtrsim 3700$ K implies that, for certain ranges of $D_{\rm ac}$ and T_Q, the point where the curves cross may be ambiguous over a range of a few hundred K, yielding poorly defined T_S and f_S values.

4.2. *Error Analysis for Derived T_S and f_S Values*

We estimated uncertainties in the derived starspot parameters seeing how the results were changed by altering various inputs to STARMOD. We expect errors in $v \sin i$ to have a negligible effect on the results, since nearly all of our data have spectral resolutions much lower than likely $v \sin i$ errors ($v \sin i$ is known to much better than ± 5 km s^{-1} for all our stars). Changing the assumed log g has a significantly greater effect. If we consider the effect on the continuum alone (through R_λ) for II Peg, using log $g = 3.0$ instead of 3.5 increases the f_S computed from the 7055 Å order by $\approx$0.03 at high T_S values to as much as 0.07 at lower T_S. At 8860 Å the effect is less, with f_S increasing by no more than 0.03 for log $g = 3$. Using log $g = 4.0$ decreases the computed f_S for high T_S but increases f_S for low T_S, with the crossover point being $\approx$3475 K for both the 7055 and 8860 Å bands. The maximum difference between f_S calculated for log $g = 4.0$, as compared to log $g = 3.5$, is 0.05 for the 7055 Å order and 0.03 for 8860 Å. When the effects on the two bands are considered together, the calculated f_S changes by less than 0.05, and T_S changes by less than 25 K in each case.

The effect on R_λ gives only part of the picture, however: the change in band depths as a function of log g is generally a larger effect. We have shown (Fig. 1 in Paper I) that TiO bands are as much as five times deeper for M giants than for M dwarfs of the same $T_{\rm eff}$. Intrinsic band depths for spots on the subgiant II Peg can be presumed to lie between those of M giants and dwarfs; the issue of whether spot spectra should be modeled by M star atmospheres of the same gravity as the active star was examined in detail in Paper II. However, the lack of a true proxy for II Peg spots (the nonexistent M subgiants) represents a fundamental limitation on the accuracy of the spot parameters derived (for any subgiant) by our TiO band methods. We find that for II Peg, the f_S yielded by fitting the TiO bands with giant spot proxy stars underestimates by up to 0.1 the f_S necessary to match contemporaneous photometry. We attribute this to lack of a spot proxy with the proper log g. Although other explanations are possible—such as contributions of plage or faculae—they need not be invoked to explain the observed discrepancy, which is due to the large change in TiO with log g. Equally, as discussed in Paper II, any possible contamination from a secondary star would be below our threshold of detection and would not explain this discrepancy. Significantly, for σ Gem, a giant active star, f_S derived from TiO bands provides a very good fit to the photometry (as in Paper II). For subgiant stars, this uncertainty should be considered as a significant source of error, underestimating f_S by perhaps $\sim$0.1 when giants are the spot proxies.

Adding random noise to the active star spectra does not measurably alter the derived f_S and T_S. When 7055 and 8860 Å band spectra of II Peg were degraded by adding S/N $\approx$ 50 G noise, changes in the measured f_S were ≤ 0.02, and the measured T_S changed by less than 25 K. As a further test, an artificial spotted star with $T_Q = 4800$ K, $T_S = 3550$ K, and $f_S = 0.5$ was created using comparison star spectra, and this was degraded by adding random noise. The maximum difference between f_S computed from the original and degraded spectra (for any initial T_Q and T_S guesses) was 0.016. Using the same T_Q and T_S used to create the spectrum, we found $f_S = 0.50$ within ± 0.005 for all S/N $\geq$ 30.

The largest source of internal error in this technique is probably the normalization of the continuum. To test this, we studied how the inferred f_S and T_S change when normalization of the active star spectrum is altered. Such a change would alter the measured band depth, vertically shifting the f_S versus T_S relations for the bands (e.g., Figs. 3 and 9) and thereby altering the deduced f_S and T_S values. To simulate the effect of incorrect normalization, we added or subtracted 0.005 (our uncertainty in Paper II) or 0.01 to all pixels redward of the band head position, using the 1995 January 19 spectrum of II Peg (where we found $f_S = 0.35$ and $T_S = 3550$ K for $T_Q = 4750$ K). Using the four possible combinations of altered spectral orders produces four (T_S, f_S) pairs having T_S values of 3480 and 3610 K and f_S of 0.31 and 0.38. This uncertainty is comparable to the differences in the f_S and T_S values yielded by fits using different nonspot comparison stars. The uncertainties quoted for our measurements in § 3 are those produced by using different nonspot comparison stars. For a ± 0.01 shift in the post-band head pixels of the II Peg spectrum, the parameter ranges increase to T_S from 3430 to 3680 K, and f_S from 0.26 to 0.41.

4.3. *Future Recommendations*

Our echelle spectra of M stars contain many bands of TiO and other molecules in addition to those used in Papers I and II. Our hope that these could extend the range of T_S over which our technique is sensitive were not realized, however, since no band in our range of wavelength coverage remained strong much above $T_{\rm eff} \approx 4000$ K. In other wavelength regions, however, there are molecular bands (such as VO and ZrO in the region between 0.9 and 1.0 μm) that could serve as diagnostics for very cool T_S. O'Neal & Neff (1997) describe the first detection of OH in starspots; infrared lines of this molecule remain strong up to $T_{\rm eff} \approx$ 4600 K. These two avenues of investigation could prove far more effective than TiO spectroscopy in extending the range of our technique's T_S sensitivity. Extending the method to $T_{\rm eff} < 3000$ K may be difficult for other reasons, though. Extremely cool giants are usually spectroscopically variable, and the difference in log g between these giants and very cool dwarfs grows with decreasing $T_{\rm eff}$, making the spot proxies even further from the optimum gravity for active subgiants.

Estimates of R_λ can be improved with new model atmospheres (e.g., Allard 1990) and/or using absolute spectrophotometry combined with *Hipparcos* parallaxes. The ultimate solution to the problem of adequate spot proxies for subgiants probably lies in direct modeling of the TiO bands (Valenti, Piskunov, & Johns-Krull 1998) using new molecular line lists (e.g., Jørgensen 1994) and model atmospheres. Doing so could eliminate the discrepancy between our computed f_S values and those best matching photometry; it would also shed light on the important question of precisely to what extent the atmospheres of starspots resemble M stars.

Future papers will focus on studies of individual active stars, with the goal of achieving nearly complete phase coverage to better constrain their starspot properties. When this is done, we hope to able to use this TiO-band method in combination with Doppler imaging to derive *morphological* constraints on starspots as well as their filling factors and temperatures. We have already begun investigations on this subject.

5. SUMMARY

We have analyzed echelle spectra of eight late-type active stars. By fitting spectral regions containing strong absorption bands of TiO, principally those near 7055 Å and at 8860 Å, we have measured starspot temperatures and filling factors on those stars. We have also measured the strengths of chromospheric emission lines and explored correlations between these strengths and starspot coverage. Obtaining high S/N observations of the 8860 Å band is critical because of the unique behavior, among the bands we have studied, of f_S derived from this band as a function of assumed T_S. By fitting a spectral order relatively unaffected by molecular bands, we have also placed spectroscopic constraints on T_Q (within ± 150 K in the best cases) for some active stars.

In four epochs of observation of II Peg, we found $T_S = 3550 \pm 100$ K. In 1995 January f_S varied between 0.26 and 0.35; in the fall of 1992 f_S varied with phase from 0.36 to 0.50. In 1991 October, f_S was approximately constant at 0.47 ± 0.02, agreeing with the low-amplitude photometric variability at that epoch. Finally, for two dates in 1995 December we found $f_S = 0.37$ and 0.40. These f_S values are likely underestimates because of the use of M giant proxies for the spots on II Peg. For EI Eri, we found $f_S = 0.30 \pm 0.08$ during 1992 March for both hemispheres, while in 1995 January one hemisphere showed no detectable spot coverage ($f_S \lesssim 0.10$) while the other had $f_S = 0.18 \pm 0.07$; in 1995 December we found $f_S = 0.15 \pm 0.06$. We were unable to determine T_S from our observations. V1762 Cyg showed $T_S = 3500 \pm 150$ K and f_S up to 0.27. HD 199178 had $f_S =$ 0.28 and 0.29 for two dates in 1994. On σ Gem, we found spot coverages ranging from ≈ 0 to 0.3 during three epochs of observation.

For II Peg, EI Eri, V1762 Cyg, HD 199178, and σ Gem, we had previously constrained T_S using single-order spectra of TiO bands; the T_S values determined here were consistent with the previous values. Three other active stars were "new" targets for this study. Three observations of DM UMa yielded $T_S = 3570 \pm 100$ K and f_S between 0.25 and 0.35, and one spectrum of HU Vir gave $T_S = 3440 \pm 100$ K and $f_S = 0.44$. Finally, on λ And we found $T_S = 3650 \pm 150$ K and f_S from ≈ 0 to 0.23.

In one case we found correlations between the strength of emission lines and starspot coverage. The lack of a strong and consistent correlation between emission strengths and f_S likely implies that spots on active stars are only sometimes spatially coincident with plage regions where emission is strongest.

D. O. was supported by grant NGT-51406 from the NASA Graduate Student Researchers Program. J. N. and D. O. were supported by NASA grant NAGW-2603 to The

Pennsylvania State University. S. S. was supported in part by NSF grant AST 95-28563 and NASA HST grant GO-06676.01-95A. This research made use of the SIMBAD database, operated by CDS, Strasbourg, France. G. Henry provided us with the original data from his photometric studies of II Peg and σ Gem. We thank the staffs of McDonald Observatory and Kitt Peak National Observatory for their allocations of observing time and for their assistance with our observations. We thank Lee Chi Wai, Alan Welty, and Larry Ramsey for their support of our observations using Penn State's Black Moshannon Observatory. It is our hope that this will not prove to be the final scientific paper using BMO data.

REFERENCES

Allard, F. 1990, Ph.D. thesis, Univ. Heidelberg
Andrews, A. D., et al. 1988, A&A, 204, 177
Barden, S. C. 1985, ApJ, 295, 162
Bessell, M. S. 1991, AJ, 101, 662
Böhm-Vitense, E. 1980, AR&A, 19, 295
Bopp, B. W., & Dempsey, R. C. 1989, PASP, 101, 516
Boyd, R. W., et al. 1983, Ap&SS, 90, 197
Butler, C. J., et al. 1987, A&A, 174, 139
Byrne, P. B., et al. 1995, A&A, 299, 115
Charles, P., Walter, F., & Bowyer, S. 1979, Nature, 282, 691
Dempsey, R. C., Bopp, B. W., Henry, G. W., & Hall, D. S. 1993a, ApJS, 86, 293
Dempsey, R. C., Linsky, J. L., Fleming, T. A., & Schmitt, J. H. M. M. 1993b, ApJS, 86, 599
Donati, J.-F., Henry, G. W., & Hall, D. S. 1995, A&A, 293, 107
Drake, S., Simon, T., & Linsky, J. L. 1989, ApJS, 71, 905
Fekel, F. C., Moffett, T. J., & Henry, G. W. 1986, ApJS, 60, 551
Gray, D. F. 1988, Lectures on Spectral Line Analysis: F, G, and K Stars (Arva, Ontario: The Publisher)
Hall, J. C., Fulton, E. E., Huenemoerder, D. P., Welty, A. D., & Neff, J. E. 1994, PASP, 106, 315
Hatzes, A. P. 1995a, AJ, 109, 350
———. 1995b, in IAU Symposium 176, Stellar Surface Structure: Poster Proceedings, ed. K. G. Strassmeier (Vienna: Inst. für Astron.), 87
Hatzes, A. P., & Vogt, S. S. 1992, MNRAS, 258, 387
Henry, G. W., Eaton, J. A., Hamer, J., & Hall, D. S. 1995, ApJS, 97, 513
Hoffleit, D., & Jaschek, C. 1982, The Bright Star Catalogue, 4th ed. (New Haven: Yale Univ. Obs.)
Huenemoerder, D. P. 1986, AJ, 92, 673
Jetsu, L., Huovelin, J., Tuominen, I., Vilhu, O., Bopp, B. W., & Piirola, V. 1990, A&A, 236, 423
Jørgensen, U. 1994, A&A, 284, 179
Johnson, H. L. 1966, ARA&A, 4, 193
Kimble, R. A., Kahn, S. M., & Bowyer, S. 1981, ApJ, 251, 585
Kurucz, R. L. 1991, in Precision Photometry: Astrophysics of the Galaxy, ed. P. Davis, A. Upgren, & K. Janes (Schenectady: L. Davis Press), 27
McCarthy, J. K., Sandiford, B. A., Boyd, D., & Booth, J. 1993, PASP, 105, 881
Mohin, S., & Raveendran, A. V. 1992, A&A, 256, 487
Neff, J. E., O'Neal, D., & Saar, S. H. 1995, ApJ, 452, 879 (Paper I)
O'Neal, D., & Neff, J. E. 1997, AJ, 113, 1129
O'Neal, D., Saar, S. H., & Neff, J. E. 1996, ApJ, 463, 766 (Paper II)
———. 1998, in Cool Stars, Stellar Systems, and the Sun, ed. R. Donahue & J. Bookbinder (San Francisco: ASP), CD-1439
Osten, R. A., & Saar, S. H. 1998, MNRAS, 295, 257
Piskunov, N. E., Tuominen, I., & Vilhu, O. 1990, A&A, 230, 363
Ramsey, L. W., & Huenemoerder, D. P. 1986, Proc. SPIE, 627, 282
Ridgway, S. T., Joyce, R. R., White, N. M., & Wing, R. F. 1980, ApJ, 235, 126
Rodonò, M., & Cutispoto, G. 1992, A&AS, 95, 55
Rodonò, M., et al. 1986, A&A, 165, 135
Sams, B. J., Golub, L., & Weiss, N. O. 1992, ApJ, 399, 313
Schrijver, C. J., & Zwaan, C. 1991, A&A, 251, 183
Stauffer, J. R., & Hartmann, L. W. 1986, ApJS, 61, 531
Strassmeier, K. G. 1990, ApJ, 348, 682
———. 1994, A&A, 281, 395
Strassmeier, K. G., Hall, D. S., & Henry, G. W. 1994, A&A, 282, 535
Strassmeier, K. G., et al. 1991, A&A, 247, 130
Strassmeier, K. G., Hall, D. S., Fekel, F. C., & Scheck, M. 1993, A&AS, 100, 173
Valenti, J. A., Piskunov, N., & Johns-Krull, C. M. 1998, ApJ, 498, 851
Vogt, S. S. 1981, ApJ, 247, 975
Welty, A. D., & Wade, R. A. 1995, AJ, 109, 326